Check for updates

BOREAS An international journal of Quaternary research

The last glaciation of the Arctic volcanic island Jan Mayen

ASTRID LYSÅ, EILIV A. LARSEN, JOHANNA ANJAR, NAKI AKÇAR, MORGAN GANERØD, ASBJØRN HIKSDAL, ROELANT VAN DER LELIJ AND CHRISTOF VOCKENHUBER

BOREAS

Lyså, A., Larsen, E. A., Anjar, J., Akçar, N., Ganerød, M., Hiksdal, A., Roelant Van Der Lelij & Vockenhuber, C. 2021 (January): The last glaciation of the Arctic volcanic island Jan Mayen. *Boreas*, Vol. 50, pp. 6–28. https://doi.org/10.1111/bor.12482. ISSN 0300-9483.

The volcanic island of Jan Mayen, remotely located in the Norwegian-Greenland Sea, was covered by a contiguous ice cap during the Late Weichselian. Until now, it has been disputed whether parts of the island south of the presently glaciated Mount Beerenberg area were ever glaciated. Based on extensive field mapping we demonstrate that an ice cap covered all land areas and likely also extended onto the shallow shelf areas southeast and east of the island. Chronological interpretations are based on K-Ar and $^{40}Ar/^{39}Ar$ dating of volcanic rocks, cosmogenic nuclide (^{36}Cl) surface exposure dating of bedrock and glacial erratics, and radiocarbon dating. We argue that ice growth started after 34 ka and that an initial deglaciation started some 21.5–19.5 ka in the southern and middle parts of the island. In the northern parts, closer to the present glaciers, the deglaciation might have started later, as evidenced by the establishment of vegetation 17–16 cal. ka BP. During full glaciation, the ice cap was likely thickest over the southern part of the island. This may explain a seemingly delayed deglaciation compared with the northern parts despite earlier initial deglaciation. In a broader context, the new knowledge of the Late Weichselian of the island contributes to the understanding of glaciations surrounding the North Atlantic and its climate history.

Astrid Lyså (e-mail: Astrid.Lysa@ngu.no), Eiliv A. Larsen, Morgan Ganerød, Roelant Van Der Lelij, Geological Survey of Norway, Leiv Eriksonssvei 39, Trondheim 7040, Norway; Johanna Anjar, Department of Natural Sciences and Environmental Health, University of South-Eastern Norway, Gullbringvegen 36, Bø 3800, Norway; Naki Akçar, Institute of Geological Sciences University of Bern, Baltzerstrasse 1, Bern 3012, Switzerland; Asbjørn Hiksdal, Jadar Geotjenester AS, Kvernaland 4355, Norway; Christof Vockenhuber, Laboratory of Ion Beam Physics, ETH Zürich, Zürich 8093, Switzerland; *received 15th June 2020, accepted 2nd September 2020.*

Recently there has been substantial progress in the understanding of Weichselian ice-sheet history in the terrestrial environments of the Arctic island of Jan Mayen. Generally, the ice sheets of Greenland, Iceland, Scandinavia and Svalbard underwent a series of Weichselian glacial events and reached their maximum positions at around the time of the global glacial maximum during the last glaciation (Norðdahl & Pétursson 2005; Funder *et al.* 2011; Mangerud *et al.* 2011; Ingólfsson & Landvik 2013). Such quasi-synchronous behaviour is valid at large scales (Hughes *et al.* 2016; Stroeven *et al.* 2016); however, large variations in the age of maximum ice-marginal positions between different sectors of individual ice sheets are widely documented (Larsen *et al.* 2016). As Jan Mayen is located centrally between these four ice sheets and presently has an ice cap in the north (Figs 1, 2), it may come as a surprise that it remains unknown whether the entire island was fully glaciated during the last glaciation. This may partly be explained by the lack of focused glacial geological studies, and by the prevalence of young volcanic rocks dominating most areas of the island. Imsland (1978) concluded that Jan Mayen outside of the Beerenberg area (Fig. 2) was unglaciated during the Pleistocene, arguing against Fitch (1964) who, based on the observation of tillite beds at the foothills of Beerenberg, suggested that the island might have been glaciated. Though both researchers focused their studies on the volcanic rocks of the island, neither of their conclusions regarding Jan Mayen's glacial history was substantiated by robust data.

Although Jan Mayan is small in area, and the volume of any former ice sheet would have been insignificant compared to the Greenland Ice Sheet or Eurasian Ice Sheet, its location in relation to major ocean surface currents (Fig. 1) makes its glacial and climate history important for understanding North Atlantic palaeoclimate. As volcanic rocks on large parts of the island outside the glaciated Beerenberg area are not covered by glacigenic sediments, it has been challenging to prove or disprove the former presence of glaciers in these areas. Additionally, rough topography, rain, dense fog, and strong winds render the acquisition of accurate field observations particularly challenging. Meticulous fieldwork over the last 5 years has resulted in the documentation of sporadic occurrences of glacigenic sediments between postglacial lava flows across the island. In the northern part of Jan Mayen, Nord-Jan (Fig. 2), the situation is different. Here, the large end moraine systems that occur outside the present glaciers are interpreted to have been formed during the Little Ice Age (LIA) based on geomorphology, historical data and lichenometric dating (Anda *et al.* 1985). These authors also tentatively suggested, based on results from Iceland, that much more subdued moraines found outside of the LIA moraines may have formed some 2500 years ago.

This paper focuses on the Late Weichselian glacial history of Jan Mayen. Our main aim is to document whether the island was covered by a large glacier during the Late Weichselian. Secondary aims are to outline possible Late Weichselian glacier extents over the island,

DOI 10.1111/bor.12482 © 2020 The Authors. Boreas published by John Wiley & Sons Ltd on behalf of The Boreas Collegium
This is an open access article under the terms of the Creative Commons Attribution-NonCommercial-NoDerivs License, which permits use and distribution in any medium, provided the original work is properly cited, the use is non-commercial and no modifications or adaptations are made.

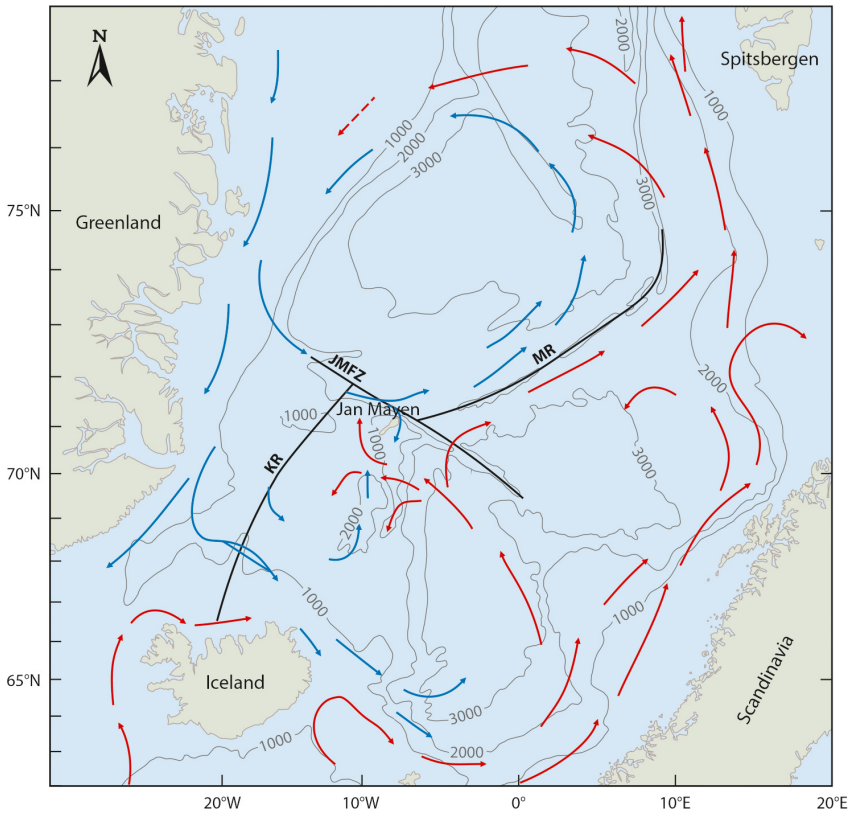

Fig. 1. Location of Jan Mayen in the Norwegian-Greenland Sea. Bathymetry is shown with 1000, 2000 and 3000 m contours. KR = Kolbeins Ridge; MR = Mohns Ridge; JMFZ = Jan Mayen Fracture Zone. Red and blue arrows indicate the main circulation patterns of the warm Atlantic and the cold Polar sea surface currents, respectively. Simplified structural features after Eldholm & Sundvor (1980). [Colour figure can be viewed at www.boreas.dk]

and to determine the age of the maximum ice-sheet configuration and subsequent deglaciation. The results are based on extensive field mapping over five field seasons, interpretation of high-resolution satellite images and a digital elevation model, radiocarbon dating, surface exposure dating using cosmogenic nuclides (^{36}Cl) on bedrock and erratics on moraines and till surfaces, and K-Ar and ^{40}Ar/^{39}Ar dating of volcanic rocks.

Setting

Jan Mayen is a volcanic island located in the Norwegian-Greenland Sea (Fig. 1). It is situated on the Jan Mayen microcontinent, which separated from East Greenland and became completely isolated around ~21.56 Ma (Blischke *et al.* 2016 and references therein). The northern end of the island is located close to the Jan Mayen Fracture Zone (JMFZ), west of the mid-oceanic Mohns spreading ridge. Significant tectonic activity along JMFZ is expressed by frequently occurring earthquakes on the island (Sørensen *et al.* 2007; Rodríguez-Pérez & Ottemöller 2014).

Jan Mayen is entirely built of volcanic rocks, mainly of potassium alkaline type (Imsland 1978). Build-up took place late in the Quaternary as evidenced by the oldest K-Ar ages of 490±120 ka in the southern part of Jan Mayen (Fitch *et al.* 1965), 460.9±55.8 ka in Midt-Jan (Cromwell *et al.* 2013), and 564±6 ka in Midt-Jan (unpublished own data). Volcanism is still active, with the most recent eruption occurring in 1985 from the Beerenberg stratovolcano (Siggerud 1986).

The rocks of Jan Mayen are divided into four stratigraphical units, three of which are exposed on land; the oldest Havhestberget formation (mainly hyaloclastites), the Nordvestkapp formation (large variety of volcanic rock types) and the youngest Inndalen formation (large variety of volcanic rock types, mostly unaffected by weathering) (Carstens 1962; Fitch 1964; Imsland 1978). Underlying these are the basement rocks, grouped as the Hidden formations.

The topography of Jan Mayen reflects the volcanic origin of the island (Figs 2B, 3A). Nord-Jan is dominated by the volcanic cone of Mount Beerenberg reaching 2277 m above sea level, which is the only known active volcano on the island. Glacier ice covers the crater and flanks of Mount Beerenberg, with some of the glacier outlets calving into the sea (Fig. 2B). Moraine ridges and other glacial deposits are found in front of the outlets and the most conspicuous moraines are suggested to be from

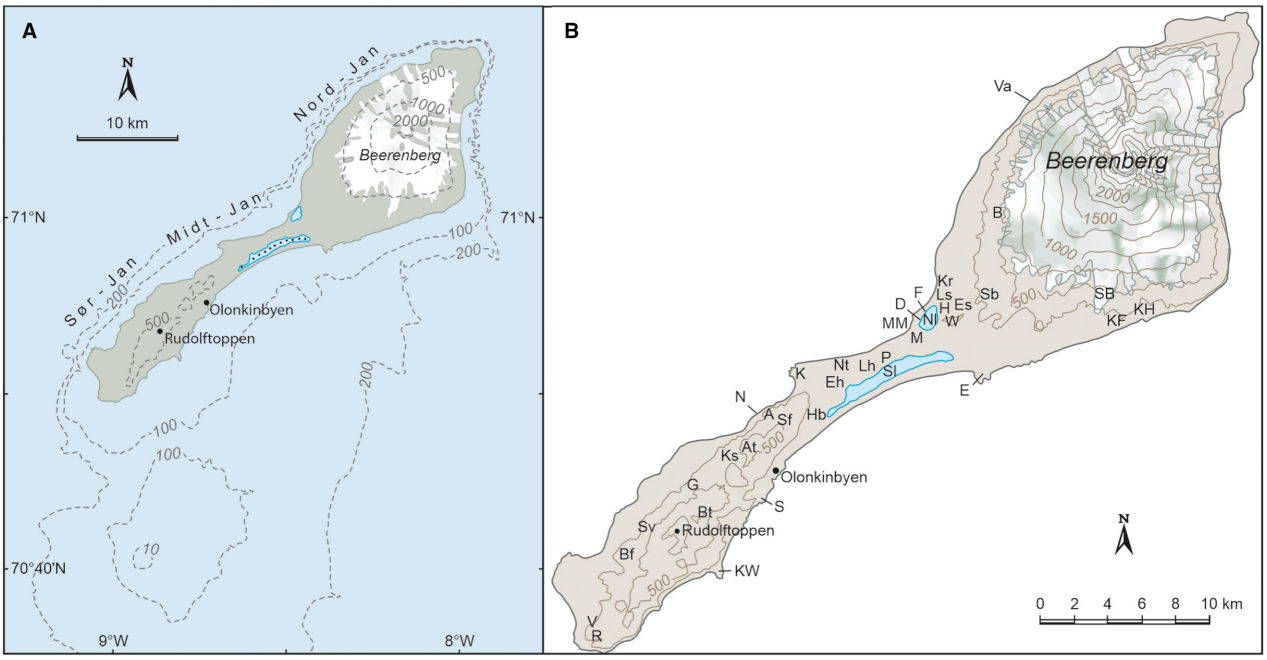

Fig. 2. A. Jan Mayen and its surrounding marine areas. Contour interval on land is 500 m. Bathymetry is shown with 100 and 200 m contours. The three main geographical areas Sør-Jan, Midt-Jan and Nord-Jan are shown, as well as the positions of the station at Olonkinbyen, the Beerenberg volcano and the highest peak in Sør-Jan, Rudolftoppen. B. Topography of Jan Mayen shown with 200 m contour interval. Place names used in the text are indicated with abbreviations: R = Ronden; V = Vøringen; Bf = Breidfjellet; Sv = Svartfjellet; KW = Kapp Wien; Bt = Blindalstoppane; G = Grovlia; S = Schiertzegga; Ks = Kubbestolen; At = Askheimtoppen; N = Nova; A = Antarcticaberget; Sf = Slettfjellet; Hb = Hannberget; K = Kvalrossen; Eh = Eimheia; Nt = Neumayertoppen; Lh = Lågheia; P = Pukkelryggen; Sl = Sørlaguna; M = Mohnberget; MM = Maria Musch bukta; Nl = Nordlaguna; D = Domen; F = Fuglefjellet; H = Hochstetter; Ls = Libergsletta; Kr = Krossbergsletta; Es = Essefjellet; Sb = Scoresbyberget; E = Eggøya; KF = Kapp Fishburn; KH = Kapp Håp; SB = Sørbreen; B = Broxrabban; Va = Vakta; W = Wildberget. [Colour figure can be viewed at www.boreas.dk]

the Little Ice Age (LIA) (Anda *et al.* 1985; Fig. 3B). Sør-Jan has a rough and variable topography dominated by numerous craters, domes, lava fields and tephra (Fig. 3A, C). A few peaks exceed 500 m a.s.l., the highest one, Rudolftoppen, reaches 769 m a.s.l. (Fig. 2). Midt-Jan connects Sør-Jan with Nord-Jan by a 2–3 km narrow land strip reaching almost 300 m a.s.l. Craters and tephra also exist in Midt-Jan (Fig. 3D).

The onshore rugged topography is also reflected in very variable offshore water depths. Shallow banks surround the island to the south and east with water depths less than 200 m over wide areas (Fig. 2A), suggesting that large areas to the south and southeast may have been subaerially exposed during the Last Glacial Maximum (LGM) eustatic sea-level lowstand (Clark & Tarasov 2014). Beyond the northern coast, water depths of more than 2000 m are rapidly attained (cf. Figs 1, 2A).

Freshwater is scarce on the island. The only permanent lake is the almost 40 m deep lake Nordlaguna on the western coast, whereas the Sørlaguna (lagoon) on the eastern coast is only periodically filled with shallow water (Fig. 2B). Apart from this, fresh water occurs mainly as meltwater in front of the largest glacier outlets or as temporary rivers active during heavy rainfall and snowmelt.

The present climate of Jan Mayen is influenced by both Atlantic surface water-masses entering from the south and polar water of the East Greenland Current entering from the north (Fig. 1). The climate is Arctic-maritime with cool summers and mild winters. The current average annual temperature is close to 1 °C at sea level, which is higher than during the latter part of the last century when it was below 0 °C (Hudson *et al.* 2019). Sea ice has not been observed around the island since the late 1990s according to personnel at the Jan Mayen station, which corresponds with observed decreasing sea-ice extent in Fram Strait and in the Barents Sea since the late 1970s (Polyak *et al.* 2010; MOSJ Homepage 2019).

Material and methods

Extensive fieldwork was carried out during 2014 to 2018. Multiple data sets, including ArcticDEM (Porter *et al.* 2018), elevation data from the Norwegian Polar Institute (40-m contour interval), and satellite images (panchromatic and multispectral from 2011 to 2013) provided by Kongsberg Satellite Services, were analysed mainly to supplement the field mapping. All sites were georeferenced using GPS and later processed using ArcGIS 10.6. Sites were sampled and documented using photography and detailed descriptions, e.g. surface-texture and mor-

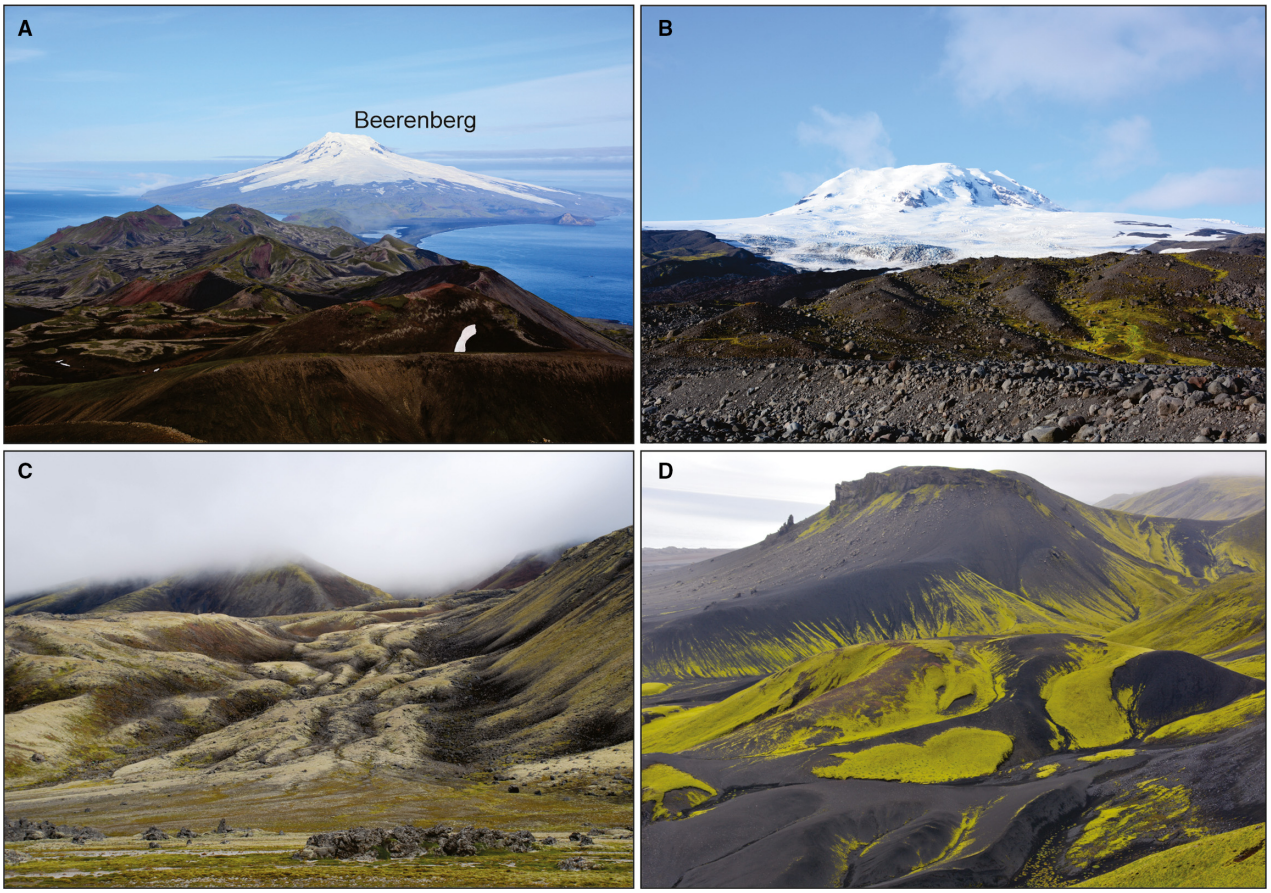

Fig. 3. A. View from the highest peak of Sør-Jan, Rudolftoppen, towards Beerenberg. Volcanic craters, domes, lava fields and tephra fall dominate the landscape in Sør-Jan. B. LIA moraine ridges in front of the Sørbreen glacier outlet. Beerenberg in the background. C. Postglacial lava flow NE of Grovlia. D. Tephra in Midt-Jan, close to Hannberget. [Colour figure can be viewed at www.boreas.dk]

phology description and lithostratigraphical logging. Local place names are shown in Fig. 2B.

$^{40}Ar/^{39}Ar$ and K-Ar dating

Two to four samples of basaltic rocks were collected from each lava flow for $^{40}Ar/^{39}Ar$ and K-Ar analyses (Table 1, Table S1). Given the young nature of these rocks, this strategy was chosen to test the analytical reproducibility. The samples were crushed and sieved into 180–250 μm fractions at the Geological Survey of Norway. Only groundmass was considered suitable for analysis. The samples were packed in aluminium capsules together with the Adler Creek Rhyolite (AC) flux monitor standard along with pure (zero age) K_2SO_4 and CaF_2 salts. The samples were irradiated at the Institute for Energy Technology, Kjeller, Norway with a nominal neutron (n) flux of 1.3×10^{13} n cm^{-2} s^{-1} for 2 h, which gives an approximate fluence of 9.36×10^{16} n cm^{-2}. The raw mass spectrometer data and interference correction factors (from K and Ca) can be found in Table S1. Due to the low level of ^{36}Ar in these young samples, careful monitoring of changes of the mass bias and blanks were undertaken. Mass bias (+ blank) was measured before each unknown (+ blank). We used an interpolated mass bias ratio into the unknown using a spline fit. The rest of the analytical procedures follow Plunder *et al.* (2020).

K-Ar analyses followed standard isotope dilution procedures at the Geological Survey of Norway. Samples were crushed to 180–300 μm and packed in Mo foil. The samples were degassed at 1400 °C for 20 min, and spiked with a known amount of pure ^{38}Ar. Spiked gas was purified using a combination of a Ti sublimation pump and SAES ST-101 getter cartridges, and analysed on an IsotopX NGX multicollector noble gas mass spectrometer. Mass discrimination was corrected using an online air pipette and the atmospheric composition of Lee *et al.* (2006). K was determined by dissolving Li-tetraborate fluxed sample in HNO_3 spiked with Rh as an internal standard and analysing on a Perkin Elmer 4300 DV ICP-OES. Ages were calculated using the decay constants of Steiger & Jäger (1977). Uncertainties were propagated using the error propagation model of Hałas & Wójtowicz (2014). The assessment of reliability for K-Ar ages was

Table 1. K-Ar and $^{40}Ar/^{39}Ar$ ages. Main age data result from K-Ar and $^{40}Ar/^{39}Ar$ geochronology. See Table S1 for more information.

Sample no.	Site	Geographical position	K-Ar (ka)±2σ	$^{40}Ar/^{39}$ Ar (ka)±2σ	Concluded age (ka)±2σ	Comments
JM2015-16	JM49A Kapp Fishburn	N70° 59.721′ W8° 11.177′	71.7±6.2	65.6±20	58.6±6.1	Both methods are consistent. The oldest K-Ar date is likely too old.
JM2015-17			60.5±6.8	No result		
JM2015-18			63.4±5.4	No result		
JM2015-19			53.5±5	No result		
JM2015-20	JM49B Kapp Fishburn	N70° 59.721′ W8° 11.177′	58.9±5.4	69.4±17.4	60.0±3.0	Oldest $^{40}Ar/^{39}Ar$ is likely too old.
JM2015-21			65.8±4.8	112.7±30.0		
JM2015-22			52.9±5.8	43.5±23.0		
JM2017-17A	JM08 Kapp Fishburn (dyke)	N70° 59.793′ W8° 09.881′	23.5±3.2	Not analysed	25.4±2.4	Weighted mean of K-Ar dates.
JM2017-17B			28.9±4.4			
JM2017-17C			25.2±4.4			
JM2015-35	JM57 Kapp Håp	N71° 00.204′ W8° 08.076′	47.0±6.6	49.0±59	47.6±6.3	JM2015-37 and 38 have problematic behaviour and are not included.
JM2015-36			72.8±6.6	55.0±24		
JM2015-37			33.9±6.6	No result		
			31.1±5.0			
JM2015-38			34.5±6.8	No result		
JM2015-45	JM68 Domen	N70° 59.822′ W8° 29.940′	19.2±3.8	Not analysed	21.5±2.6	Weighted mean of K-Ar dates.
JM2015-46			23.6±3.4			
JM2015-69	JM81 Fugleberget	N71° 00.357′ W8° 29.121′	103.0±5.2	61.0±9.8	76.2±3.4	Two K-Ar and 1 combined normal isochron $^{40}Ar/^{39}Ar$ (75.4±7.5).
JM2015-70			77.1±4.8	No result		
JM2015-71			75.1±6.6	77.0±9.8		
JM2015-72			87.7±6.4	67.0±12.1		

based on the reproducibility of multiple K-Ar samples from each site.

^{36}Cl cosmogenic surface exposure dating

Samples for ^{36}Cl cosmogenic surface exposure dating were collected from erratic boulders on till surfaces and from glacially abraded bedrock surfaces using a hammer and chisel (field season 2014) and an electrical rock saw (field seasons 2015 and 2016) (Table 2). All boulders were carefully assessed for possible rotation and postdepositional movements (including earthquake tremors) before sampling, preferably from flat areas. As far as possible, 2–3 erratics were sampled from the same till area, preferably at different elevations. Bedrock was sampled where suitable boulders were lacking. Sample locations and altitudes were recorded using a GPS. As far as the foggy climate permitted, topographic shielding at each sampling location was measured with a clinometer and compass and calculated following Dunne *et al.* (1999).

The samples were processed at the Institute of Geological Sciences, University of Bern following the protocol described in Mozafari *et al.* (2019). The samples were crushed to a grain size of 250–400 μm and the crushed whole-rock samples were leached in diluted HNO_3 and rinsed with ultrapure water. Subsamples for elemental analysis were sent to Activation laboratories, Canada, where major elements and important trace elements were measured (Table S2). After leaching, 30 g of each sample was dissolved in a mixture of HF and HNO_3 together with 2.5 mg of enriched ^{35}Cl spike. $AgNO_3$ was then added and the chlorine was precipitated as AgCl and filtered by centrifugation. The ^{36}S, which is the isobar of cosmogenic ^{36}Cl, was then removed by $BaSO_4$ precipitation. Total Cl and ^{36}Cl concentrations were measured by accelerator mass spectrometry (AMS) at the ETH 6 MV Tandem accelerator facility in Zurich, Switzerland (Ivy-Ochs *et al.* 2004; Christl *et al.* 2013; Vockenhuber *et al.* 2019). The isobar ^{36}S was removed by the method of the gas-filled magnet and identified in the gas ionization detector (Vockenhuber *et al.* 2019). The remaining sulphur correction of the measured $^{36}Cl/^{35}Cl$ ratio was insignificant. The measured $^{36}Cl/^{35}Cl$ ratios were then normalized to the ETH internal standard K382/4N with a value of $^{36}Cl/^{35}Cl$ of $(17.36\pm0.35)\times10^{-12}$ (Christl *et al.* 2013). Finally, measured $^{36}Cl/^{35}Cl$ ratios were corrected for a full process blank ratio of $(3\pm2)\times10^{-15}$, which resulted in a blank correction for the samples of a few percent. The exposure ages were calculated using the CRONUScalc web-interface (Marrero *et al.* 2016) and LM scaling.

Two radiocarbon ages relevant for this study were obtained (Table 3). One conventional date, previously unpublished, was obtained in the 1970s from the National Laboratory for Age Determination in Trondheim (Norway) from sample T-3991B. The other date was obtained by AMS at the Radiocarbon Dating Laboratory, Department of Geology (Lund University, Sweden) from sample LuS 12204. The dates were

Table 2. ^{36}Cl cosmogenic surface exposure ages.

Sample no.	Site	Geographical position	Elevation (m a.s.l.)	Sampled	Sample thickness (cm)	Shielding[1]	Concentration of chlorine in the rock (ppm)	^{36}Cl concentration (^{36}Cl 10^6 g^{-1})	Cosmogenic Cl (10^6 atoms g^{-1} sample)	Radiogenic Cl (10^6 atoms g^{-1} sample)	Age (ka)[2]
JM2014-01	JM02 Lågheia	N70° 58.507′ W8° 37.230′	114	Bedrock	2	0.987	24.17	0.161	0.159	0.002	19.7±1.7 (1.1)
JM2014-02	JM03 W of Sørbreen	N70° 59.732′ W8° 15.424′	116	Bedrock	3	0.997	17.38	0.114	0.114	0.000	14.3±1.5 (1.0)
JM2014-03	JM04 W of Sørbreen	N70° 59.823′ W8° 15.166′	140	Bedrock	4.5	0.996	67.38	0.130	0.128	0.002	13.4±1.4 (1.0)
JM2014-04	JM05 W of Sørbreen	N70° 59.854′ W8° 15.091′	144	Block on till	3.5	0.997	129.93	0.142	0.139	0.002	12.6±1.5 (1.0)
JM2014-19	JM21 Essefjellet	N71° 00.623 W8° 26.003′	120	Bedrock	1.5	0.996	16.08	0.117	0.117	0.000	13.6±1.3 (0.9)
JM2014-20	JM22 Essefjellet	N71° 00.736′ W8° 25.358′	144	Bedrock	1.5	0.999	43.53	0.117	0.116	0.001	12.1±1.2 (0.9)
JM2014-21	JM24 Essefjellet	N71° 00.776′ W8° 24.726′	162	Block on till	1.5	0.997	15.67	0.163	0.163	0.000	19.2±2.5 (2.2)
JM2014-23	JM26 Mohnberget	N70° 59.378′ W8° 29.803′	71	Bedrock	3	0.999	19.43	0.161	0.159	0.002	19.8±1.8 (1.3)
JM2015-73	JM83 Kapp Wien	N70° 52.040′ W8° 48.549′	45	Block on till	1.7	0.980	62.30	0.091	0.072	0.019	7.9±1.6 (1.5)
JM2015-74	JM84 Kapp Wien	N70° 52.080′ W8° 48.372′	32	Block on till	1.5	0.996	108.32	0.149	0.113	0.036	10.6±1.6 (1.2)
JM2015-99	JM95 Lågheia	N70° 58.243′ W8° 36.070′	115	Block on till	1.8	1.000	27.21	0.084	0.081	0.003	10.0±1.5 (1.4)
JM2015-100	JM96 Lågheia	N70° 58.403′ W8° 36.510′	109	Block on till	1.5	1.000	29.61	0.021	0.018	0.003	2.2±3.1 (3.1)
JM2015-101	JM97 Lågheia	N70° 58.396′ W8° 36.567′	100	Block on till	2	1.000	32.28	0.100	0.097	0.003	12.3±1.8 (1.6)
JM2016-22	JM128 Svartfjellet	N70° 53.753′ W8° 55.596′	340	Block on till	1.5	0.997	48.16	0.227	0.221	0.006	19.3±2.5 (2.1)
JM2016-23	JM129 Svartfjellet	N70° 53.546′ W8° 54.821′	412	Bedrock	1.6	0.996	19.19	0.187	0.185	0.002	17.0±2.0 (1.7)
JM2016-24	JM131 Svartfjellet	N70° 53.361′ W8° 54.876′	437	Block on till	2	0.993	196.72	0.275	0.239	0.036	13.1±2.6 (2.0)
JM2016-25	JM132 Svartfjellet	N70° 53.544′ W8° 55.822′	258	Block on till	1.5	0.996	64.07	0.222	0.215	0.008	19.2±2.5 (2.1)
JM2016-26	JM133 Svartfjellet	N70° 53.539′ W8° 55.800′	258	Block on till	1.5	0.997	85.38	0.229	0.219	0.010	18.9±2.7 (2.1)
JM2016-29	JM142 W of Askheimtoppen	N70° 55.684′ W8° 46.296′	397	Block on till	1.5	0.998	99.47	0.185	0.168	0.017	12.0±2.0 (1.7)
JM2016-30	JM144 W of Askheimtoppen	N70° 55.719′ W8° 46.448′	366	Block on till	1.2	0.992	21.23	0.120	0.117	0.003	11.2±1.5 (1.3)
JM2016-31	JM151 Slettfjellet	N70° 57.487′ W8° 40.824′	265	Block on till	1.2	0.998	32.90	0.142	0.138	0.004	13.8±1.5 (1.2)
JM2016-32	JM155 Slettfjellet	N70° 57.005′ W8° 42.220′	337	Block on till	2.4	0.992	218.60	0.299	0.248	0.051	13.8±2.5 (1.7)

(continues)

Table 2. (continued)

Sample no.	Site	Geographical position	Elevation (m a.s.l.)	Sampled	Sample thickness (cm)	Shielding[1]	Concentration of chlorine in the rock (ppm)	^{36}Cl concentration (^{36}Cl 10^6 g^{-1})	Cosmogenic Cl (10^6 atoms g^{-1} sample)	Radiogenic Cl (10^6 atoms g^{-1} sample)	Age (ka)[2]
JM2016-33	JM162 Antarcticaberget	N70° 57.080′ W8° 44.536′	202	Bedrock	1.2	0.994	27.24	0.123	0.119	0.004	13.2±1.6 (1.4)
JM2016-34	JM164 Antarcticaberget	N70° 57.116′ W8° 44.209′	217	Block on till	2.3	0.999	69.73	0.129	0.119	0.010	11.3±2.4 (2.2)
JM2016-35	JM167 Slettfjellet	N70° 57.049′ W8° 41.433′	318	Block on till	1.8	0.999	19.94	0.132	0.130	0.002	13.5±1.4 (1.1)
JM2016-39	JM178 Kapp Wien	N70° 52.193′ W8° 49.084′	126	Block on till	1.8	0.992	65.61	0.115	0.097	0.018	9.4±1.7 (1.5)
JM2016-40	JM198 NW of Kubbestolen	N70° 55.801′ W8° 48.952′	205	Block on till	1	0.994	25.88	0.099	0.096	0.002	11.5±1.7 (1.5)
JM2016-42	JM203 Breidfjellet	N70° 52.655′ W8° 57.171′	321	Block on till	1	0.999	15.05	0.235	0.234	0.001	23.1±3.6 (3.3)

[1]Shielding only includes topographic shielding, no correction for snow shielding.
[2]Calculated using LM scaling and assuming zero erosion. Bulk density assumed to be 2.1±0.3 g cm^{-3} based on Icelandic basalt samples (Licciardi *et al.* 2008). See Table S2 for composition of the samples. Calculated using the CRONUS web calculator: http://cronus.cosmogenicnuclides.rocks/2.0/html/cl/

calibrated using CALIB 7.1 (Stuiver *et al.* 2019) and the IntCal13 calibration data set (Reimer *et al.* 2013).

Results

Since prior to this study it was unknown whether the entire island had ever been glaciated (Fitch 1964; Imsland 1978), extensive fieldwork was completed to address this question. As postglacial volcanic activity has affected large areas in Jan Mayen, sites with older bedrock (Fig. 4) were specifically targeted. The results are presented for three sub-regions: Nord-Jan, Midt-Jan and Sør-Jan (Fig. 2A), where we mapped till covers, ice-marginal moraines, glacial striations, and glacial meltwater channels, in areas unaffected by younger volcanic strata.

Nord-Jan

Nord-Jan is dominated by the majestic glacier-covered stratovolcano Mount Beerenberg (Figs 2, 3A). Moraines interpreted to have been formed during the Little Ice Age and Late Holocene, based on historical data and lichenometric dating, are found near the present glacier margins (Anda *et al.* 1985). Outside these, till typically occurs on lower plains close to sea level and between valleys, hills and lava flows on higher surfaces (Figs 4B, 5A, B). The contrast between smooth till surfaces and adjoining younger lava surfaces is often very clear (Fig. 5C). Boulders occur in variable amounts on till surfaces and their size varies from a few dm to 1–1.5 m (Fig. 5B, D). All the boulders are subrounded and only a few exhibit clearly polished surfaces. Patterned ground (Fig. 5A, B) and solifluction lobes are widespread. In some cases, moss may make identification of till difficult, especially where boulders are absent (Fig. 5D).

A lateral moraine at the foothills of Mount Hochstetterkrateret (near Nordlaguna, Fig. 2B) is located about 5 km from the present glacier margin and only 500 m from the coastline, much farther away from present glacier margins than any other moraine in Nord-Jan, testifying to a significantly larger ice cover (Figs 5A, 6A).

Glacifluvial deposits and meltwater channels in Nord-Jan are generally associated with the present glaciers. Meltwater channels in front of glacier margins are commonly active mainly during peak melt season or during heavy rainfall. In some instances, outwash plains are also found in locations that are now abandoned by the modern drainage networks. This is the case near the Hochstetterkrateret lateral moraine described above (Fig. 6A). Just below the Scoresbyberget Mountain (Fig. 2B), meltwater channels eroded in till are located on a plateau ~120–130 m above the present meltwater system in a valley northeast of Scoresbyberget (Fig. 6B). The location and directions of these channels require a former glacier of greater extent and thickness than that during the LIA.

Table 3. Radiocarbon ages. The dates were calibrated in CALIB 7.1 (Stuiver *et al.* 2019) using the IntCal13 calibration data set (Reimer *et al.* 2013). LuS 12204 is dated by AMS whereas T-3991B is a conventional age.

Lab. code	Site	Geographical position	Dated material	Age (^{14}C a BP)	Age (cal. a BP; 68.2%)
LuS 12204	JM-NL2 Nordlaguna	N71° 00.523′ W8° 27.872′	Terrestrial plant remains, unidentified	13 670±170	17 035–16 028
T-3991B	JM84B Kapp Wien	N70° 52.080′ W8° 48.372′	Terrestrial plant remains, unidentified	9350±160	11 098–10 231

Glacially polished bedrock outcrops occur, especially close to the present glacier margin (Fig. 6C). Due to the porous nature of many volcanic rocks (Fig. 6D), well-developed striations are rare. Nevertheless, striated bedrock showing an overall radial orientation is found at several places in Nord-Jan (Fig. 7).

Midt-Jan

In Midt-Jan, tills are commonly found on nearly flat areas at different elevations underlying rocks from the Nordvestkapp and Havhestberget formations (Figs 4, 8A). Tills occur close to Mohnberget at 40–80 m a.s.l. (Fig. 8B), at Lågheia 80–220 m a.s.l. (Fig. 8C), at Eimheia 120–150 m a.s.l. (Fig. 8D) and at Slettfjellet 200–360 m a.s.l. (Fig. 8E). Generally, the till matrix is silty to sandy. Clast content varies, and the largest boulders rarely exceed 1–2 m in diameter. Many of the boulders have rounded edges indicating glacial erosion and some of them are polished (Fig. 8B, C, D). Only three sites with well-developed striations on bedrock exposures are documented in Midt-Jan (Fig. 7). The one at Nova is at the very edge of a ~125-m-high vertical coastal cliff (Figs 2B, 8F).

At Eimheia, a maximum 5-m-high, arcuate moraine ridge occurs at the base of the northeastern slope of Slettfjellet (Fig. 9A). The moraine has a very smooth surface with no boulders. A meltwater channel cuts through the southern part of the ridge.

Abandoned meltwater channels and washed till surfaces occur in several places. Cut into the till surface south of Mohnberget is a channel, up to 1.5 m deep, oriented towards Maria Musch bay (Fig. 9B). Rounded boulders and cobbles are visible at the base. The most conspicuous channel in the area originates in the flat till area of Lågheia (Fig. 9C). It runs towards the SSW, attains a depth of 2–3 m, and cuts both through till and volcanic ash before continuing south towards the coast.

At the lower part of the till-covered western slope of Pukkelryggen, a linear and narrow ridge of volcanic rocks (hyaloclastite and lava) is oriented parallel to the slope contours (Fig. 9D). The ridge is about 30 m high and about 1 km long and has a fresh and sharp appearance in contrast to the surrounding till. It is interpreted as tindar and has been formed subglacially by

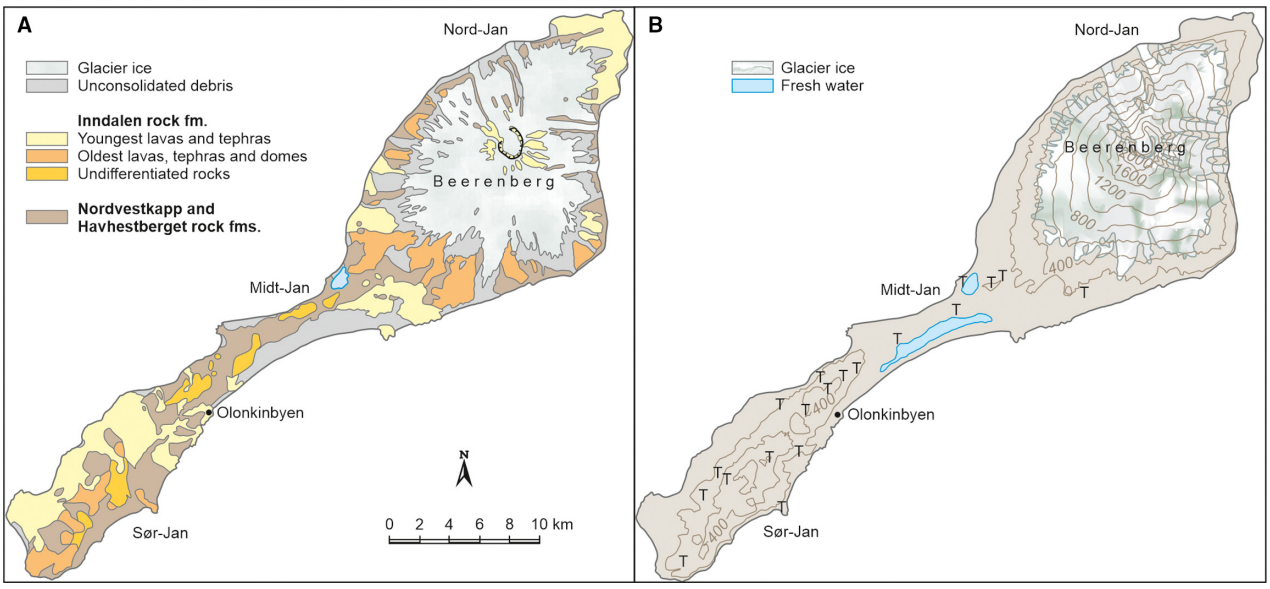

Fig. 4. A. Simplified bedrock map of Jan Mayen showing the main volcanic rock formations based on their chronostratigraphical order. The map is modified from Dallmann (1997) and based on data from Imsland (1978) and Siggerud (1972, 1986). B. Till occurrences (T). Topography is shown with 200 m contour interval. [Colour figure can be viewed at www.boreas.dk]

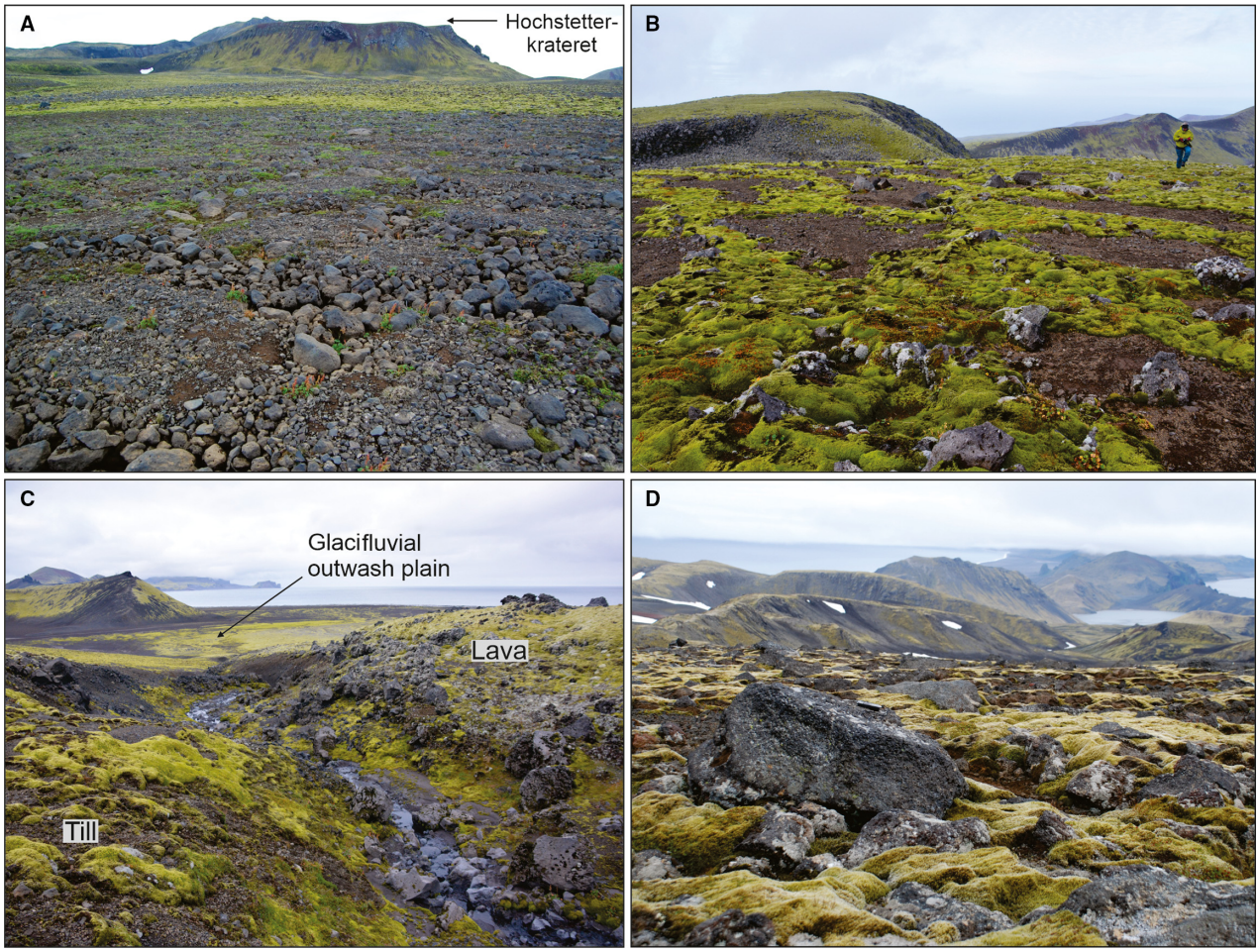

Fig. 5. Till plains in Nord-Jan. See Fig. 2B for location of sites. A. Patterned ground on till plain close to sea level at Libergsletta. B. Till cover on top of the Scoresbyberget mountain plateau. C. Smooth surface covered by till (to the left) and the rough surface of moss-covered postglacial lava (to the right) close to Krosspyntsletta. D. Boulder-rich till covered with moss at Essefjellet. The largest boulder is about 1.5 m in diameter. [Colour figure can be viewed at www.boreas.dk]

volcanic fissure eruption (e.g. Jakobsson & Gudmundsson 2008).

Sør-Jan

Sør-Jan has the most extensive postglacial lava fields and rocks of uncertain ages. Therefore, extensive traversing of the landscape was necessary to search for sites with glacigenic deposits and features.

Next to the large, northwesternmost lava flow in Sør-Jan (Fig. 4) both west and east of Kubbestolen (Fig. 2B), till is found at elevations spanning 140 to 250 m a.s.l. (Fig. 10A, B). In the lowest-lying areas to the west, the till cover is continuous with some large erratic boulders (Fig. 10A). At higher elevations to the east the till cover is discontinuous with frequently occurring bedrock exposures (Fig. 10B). Farther south, at the low-gradient western slope of Svartfjellet (Fig. 2B), till covers large areas from the 'old coastal cliff' escarpment at 200 m a.s.l. (Fig. 10C) up to about 450 m a.s.l. At this highest elevation, the till cover becomes thinner (Fig. 10D). Meltwater channels cutting into the till originate at higher elevations and run perpendicular to the contours towards the coast. Some channels are up to 2–3 m deep and 3–5 m wide (e.g. Fig. 10D). The channels are visible on satellite images, in which the contrast between the smooth till surface and younger lava is clearly visible (Fig. 10E).

In the southernmost part of Jan Mayen, at elevations between 50 and 250 m a.s.l., thick till covers the smooth and low-gradient areas close to Vøringen and Ronden (Figs 2B, 4B, 11A, B). Thick moss often prevents closer observations. In places, however, erratic boulders are found. Where exposed, the till matrix is found to be sandy. Patterned ground and solifluction lobes are common where till covers the ground.

On top of the sea cliff at Kapp Wien in the southeast part of the island (Fig. 2B), a thin cover of sandy till occurs at elevations spanning 20 to 120 m a.s.l. The surface is smooth with few erratic boulders. A stratigraphical section in the cliff exposes a sedimentary succession and under-

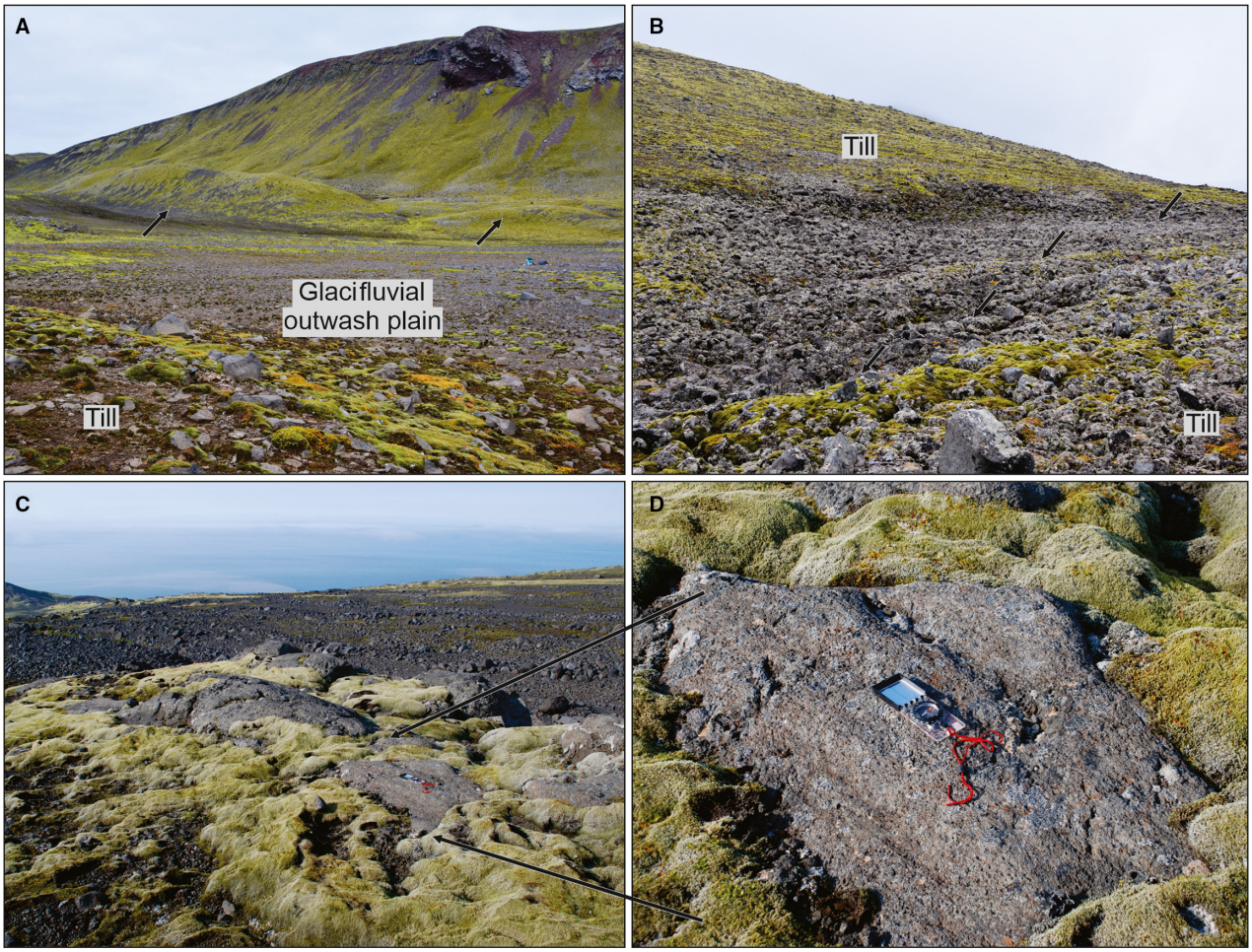

Fig. 6. Glacial features in Nord-Jan. For location of sites, see Fig. 2B. A. Outwash plain and lateral moraine (black arrows, see also Fig. 5A) near Hochstetterkrateret and Libergsletta. B. Meltwater channels (black arrows) eroded into till next to the Scoresbyberget mountain. C. Fluted till surface and glacier-polished bedrock (roche moutonnè) close to the present glacial margin at Broxrabban. D. Close-up of the glacier-polished bedrock surface in C showing striations of the porous volcanic rock. Compass for scale. [Colour figure can be viewed at www.boreas.dk]

lying volcanic rock (Fig. 11C). It shows from the base upwards an approximately 1-m-thick till covered by volcanic ash, lapilli and a thin horizon containing organic material. A thin till occurs at the top of the section.

The almost flat and smooth surface of Blindalstoppane (636 m a.s.l.) (Fig. 2B) consists of sandy gravelly till (Fig. 11D). Polished pebbles are found, as well as a few boulders with maximum diameters of about 60 cm.

Chronology

K-Ar and $^{40}Ar/^{39}Ar$ ages

Volcanic rocks underlying till or interpreted to have been erupted during the last glaciation or deglaciation were selected for K-Ar and $^{40}Ar/^{39}Ar$ dating (Fig. 12, Table 1). Rocks underlying surficial till in Nord-Jan (coastal cliff at sites JM49, Kapp Fishburn and JM57, Kapp Håp) yielded ages of 47.6±6.3, 58.6±6.1 and 60.0±6.6 ka (Fig. 13). Volcanic dykes extending vertically towards the surface (i.e. coastal cliff at site JM08, Kapp Fishburn) are covered by till at the surface, and yielded an age of 25.4±2.4 ka (Fig. 13). These dykes were emplaced after the eruption that formed the major cliffs at Kapp Fishburn and Kapp Håp and were likely formed subglacially. In Midt-Jan basalt below till (Fugleberget, site JM81) yielded an age of 76.2±3.4 ka (Fig. 13). Adjacent to this sample site, the pinnacle of Domen (site JM68) exhibits a fresh and jagged topography. In Domen there is a transition from subglacially formed hyaloclastite to subaerial lava, both resulting from the same eruption. Thus, this eruption started beneath glacier ice before protruding through the glacier surface. A dyke formed during this eruption was dated to 21.5±2.6 ka (Fig. 13).

Cosmogenic exposure ages

Erratic boulders and glacially eroded bedrock were sampled for TCN dating (Fig. 12, Table 2). All sites in

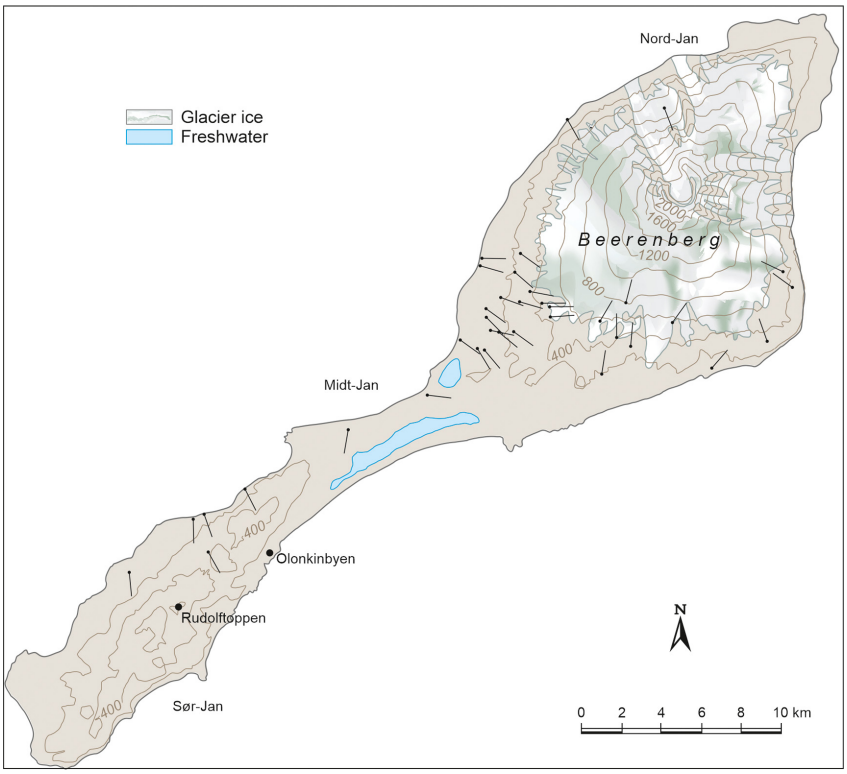

Fig. 7. Directions of glacial striations. Ice movement direction towards the head. Head also marks site location. Topography is shown with 200 m contour interval. [Colour figure can be viewed at www.boreas.dk]

Sør-Jan and Midt-Jan, i.e. sites from areas where past ice cover has previously not been confirmed (Fitch 1964; Imsland 1978), are included in this study. In Nord-Jan only sites from the southwestern part of the region, i.e. most distal to presently glaciated areas, are reported here. Areas proximal to the presently glaciated Mount Beerenberg will be discussed in a separate paper focusing on Lateglacial and Holocene glacier variations. The TCN dates are plotted separately for the three regions vs. elevations above sea level (Fig. 14).

In Sør-Jan the cosmogenic exposure ages range between 23.1±3.6 and 7.9±1.6 ka. The oldest ages are from Breidfjellet and Svartfjellet (Fig. 2B), at elevations between ~250 and 350 m a.s.l. There is a trend towards slightly younger ages with higher elevation amongst these mountains, although the youngest ages obtained are from the Kapp Wien site (Fig. 2B) at ~130 and 30 m a.s.l.

In Midt-Jan the oldest ages of 19.8±1.8 to 19.7±1.7 ka are from sites at low elevations (Mohnberget and Lågheia, Fig. 2B). These two dates are both from bedrock exposures. At Lågheia, two additional samples from blocks resting on till yielded ages of 12.3±1.8 and 10.1±1.5 ka. Another sample yielded an anomalously low age of around 2.2 ka. At Slettfjellet and Antarcticaberget, from elevations above ~200 m a.s.l., ages span 13.8±2.5 to 11.3±2.4 ka (Fig. 2B).

In Nord-Jan the oldest age of 19.2±2.5 ka was obtained from the Essefjellet area, 160 m a.s.l. (Fig. 2B), whereas all the other dates are from slightly lower elevations and span 14.3±1.5 to 12.1±1.2 ka.

Radiocarbon ages

Radiocarbon ages were obtained from only two sites (Fig. 12, Table 3). The lake Nordlaguna (Fig. 2B) age of 16 028–17 035 cal. a BP from sample JM-NL2 is from resedimented plant fragments collected from the lower part of a sediment core in Nordlaguna. At Kapp Wien, unidentified organic material collected from volcanic deposits ~2.5 m below the uppermost till was dated (site JM84B, Figs 2B, 11C) in the 1970s but remained unpublished. The calibrated age of this sample, 10 231–11 098 cal. a BP, is close to the oldest TCN age from this site (10.6±1.6 ka; Fig. 14), the implications of which are discussed below.

Discussion

Ice cap over Jan Mayen

Glacier ice constitutes about 30% of the island's total area (Orheim 1993) and some outlet glaciers extend all the way down to present sea level. Still, it has been questioned whether the middle and southern parts of the island have ever been glaciated (Imsland 1978). These conflicting views partially arose from the extensive

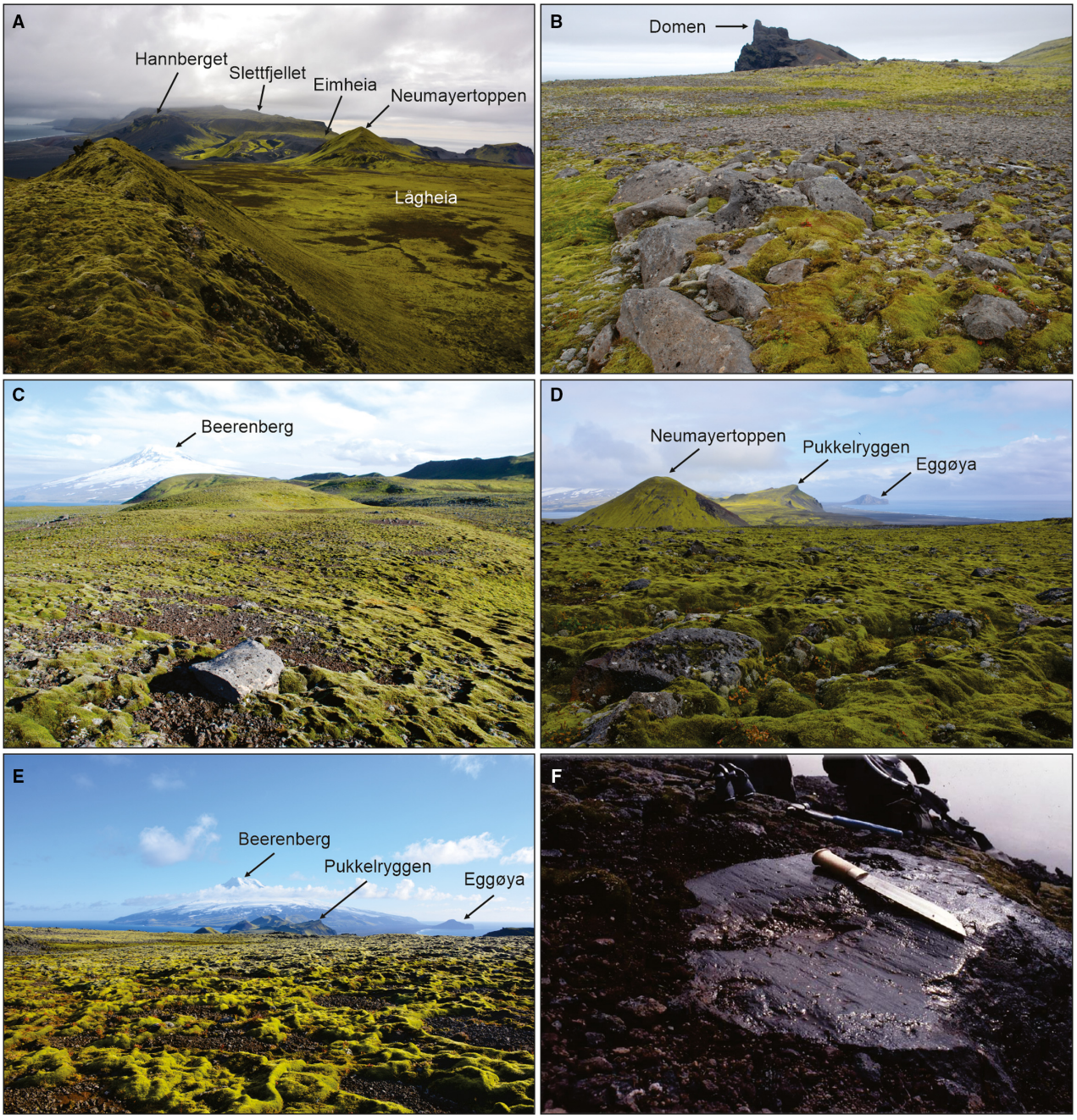

Fig. 8. Till plains and glacial features in Midt-Jan. For location of sites, see Fig. 2B. A. Overview of the plateau areas Lågheia, Eimheia and Slettfjellet of Midt-Jan covered by till. Southwestward view from Pukkelryggen. B. Till cover at Mohnberget. C. Striated boulder at the till surface at Lågheia. D. Till covered with moss at Eimheia. E. Till cover at Slettfjellet. Note the very flat surface and near absence of large cobbles. F. Striations on bedrock at the coastal cliff of Antarcticaberget. Knife is about 35 cm long. [Colour figure can be viewed at www.boreas.dk]

postglacial volcanism but were compounded by a lack of systematic glacial geological studies until now. We have mapped till, glacial erratics, glacial striae and meltwater channels over large parts of the island (e.g. Figs 4B, 7). The extent of till in Nord-Jan indicates that glacier ice formerly extended over the plains to the present coastline (e.g. Fig. 5A). Till is also located on isolated mountain plateaus above 300 m a.s.l. (e.g. at Essefjellet, Scoresbyberget and Wildberget, Fig. 5B, D). Similarly, meltwater channels are situated 120–130 m above present proglacial meltwater systems (at Scoresbyberget, Fig. 6B). These observations suggest that glacier ice formerly extended at least to the present coastline, and that these glaciers were much thicker than those extending to

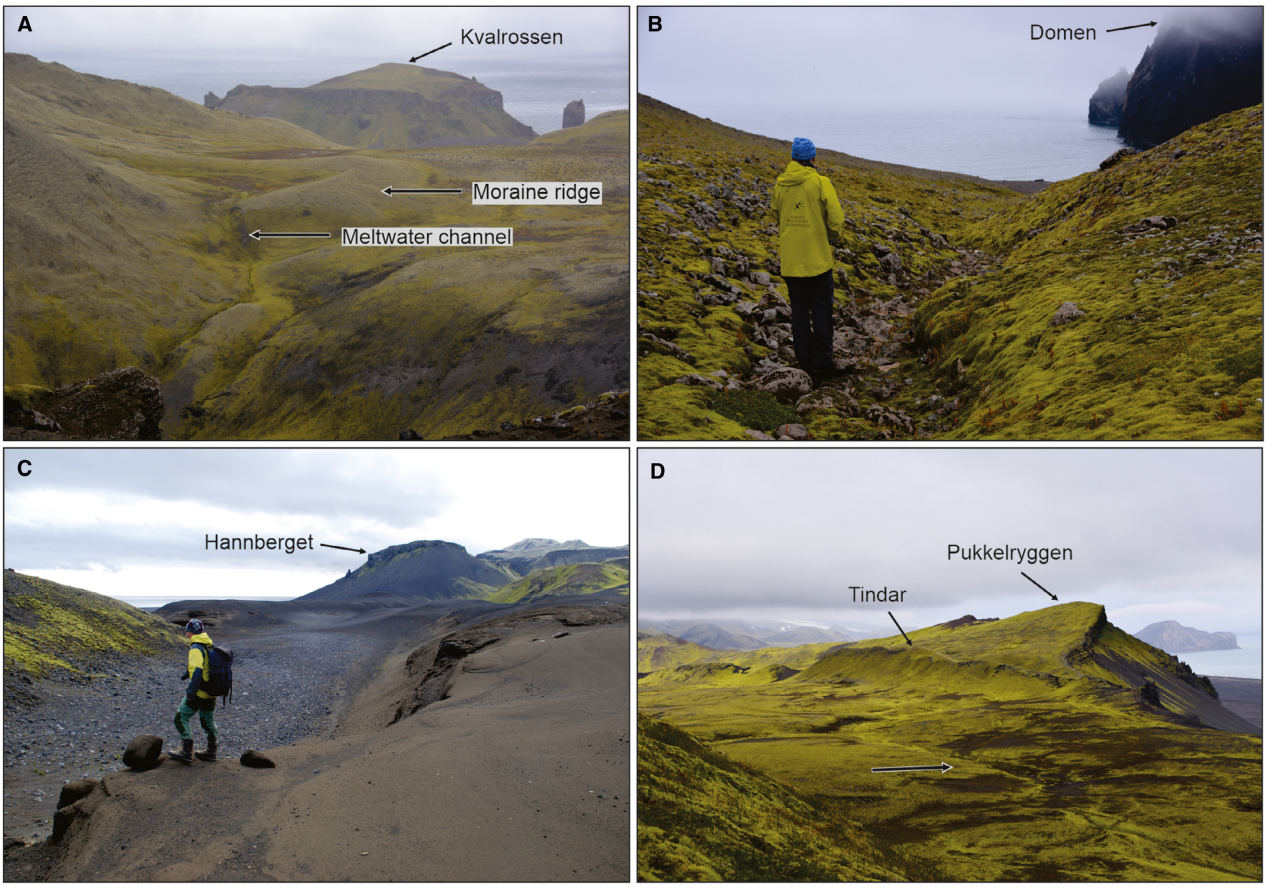

Fig. 9. Glacial features in Midt-Jan. For location of sites, see Fig. 2B. A. Arcuate moraine ridge incised by a meltwater channel at Eimheia. B. Abandoned meltwater channel with a lag of rounded cobbles and boulders draining towards the bay of Maria Musch. C. 2 to 3 m deep abandoned meltwater channel at Lågheia incised through volcanic ash. Person for scale. D. Tindar close to Pukkelryggen, Lågheia. black arrow indicates the start area of the abandoned meltwater channel shown in C. View from Neumayertoppen. [Colour figure can be viewed at www.boreas.dk]]

Holocene moraines in the southeastern part of Nord-Jan.

In Midt-Jan till is ubiquitous in areas containing volcanic rocks belonging to the Nordvestkapp and Havhestberget formations (Fig. 4). The occurrence of till over large, rather levelled areas at different elevations (Fig. 8A) indicates a formerly thick, continuous ice cover. The till at Slettfjellet (Fig. 8A, E) extends to the edge of the ~200-m-high coastal cliff at Antarcticaberget, where striated bedrock is exposed (Fig. 8F). This till mantling the west coast, along with till at Pukkelryggen on the east coast (Fig. 9D), supports the notion of a formerly continuous ice cover extending to at least the present coastline.

Abandoned meltwater channels in both Midt- and Sør-Jan also record former glacier extents. These channels commonly occur in locations and at elevations that cannot be explained without the former presence of melting glacier ice and additionally, they may indicate earlier periods of significant erosion (e.g. Figs 9C, 10D, E). The subglacially formed volcanic tindar close to Pukkelryggen, which rises to about 230 m a.s.l. (Fig. 9D), also clearly indicates a once continuous and thick ice cover over the island.

Similarly as in Midt-Jan, till deposits in Sør-Jan mainly occur on rocks from the Nordvestkapp and Havhestberget formations and, in some cases on the oldest strata of the Inndalen formation (Figs 4, 11A, B, C). Till and other glacial landforms and sediments occur at coastal cliffs and plateaus at differing elevations (Figs 10, 11), indicating that the entirety of Sør-Jan was covered by a thick glacier extending at least down to the present sea level. The highest recorded occurrence of till is at the flat area of Blindalstoppane (636 m a.s.l., Figs 2B, 11D), an area affected by strong wind deflation.

Our data strongly support the conclusion that all onshore areas (existing at the time of deglaciation) were covered by a large ice cap during the last glaciation. As one might expect striations are more abundant in Nord-Jan than in areas farther south, showing mainly a radial pattern extending from Mount Beerenberg (Fig. 7). It is noted, however, that outside the Beerenberg area, there is an absence of striae recording formerly eastward ice flow.

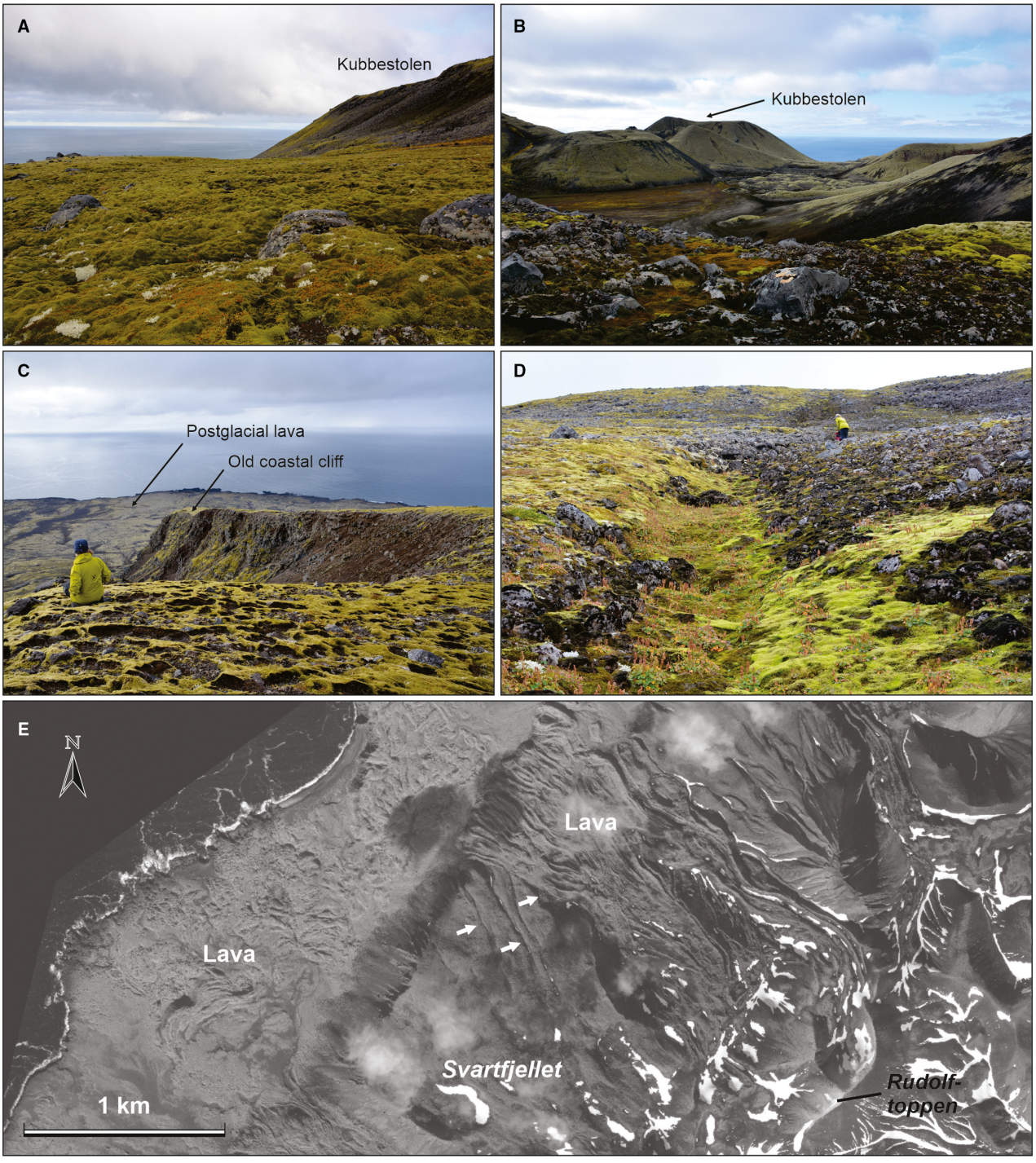

Fig. 10. Glacial deposits and features in Sør-Jan. For location of sites, see Fig. 2B. A. Surface covered by till west of Kubbestolen. B. Thin and discontinuous till east of Kubbestolen. C. Thick cover of till at the lower area of Svartfjellet. D. Meltwater channel cutting through boulder-rich till near the summit of Svartfjellet. Note that the channel originates from elevations slightly above the person. E. Smooth till-covered surface at Svartfjellet and younger lava flow in the northeast. Meltwater channels (white arrows) are visible on the till surface. Satellite image provided by Kongsberg Satellite Services AS. [Colour figure can be viewed at www.boreas.dk]

Ice cap extent and geometry

As mentioned above there is strong evidence that Jan Mayen was covered by glacier ice during the last glaciation. However, there are little data constraining former glacier extent beyond the present coastline. Judging from the available bathymetry, large areas to the south and southeast may have been subaerially

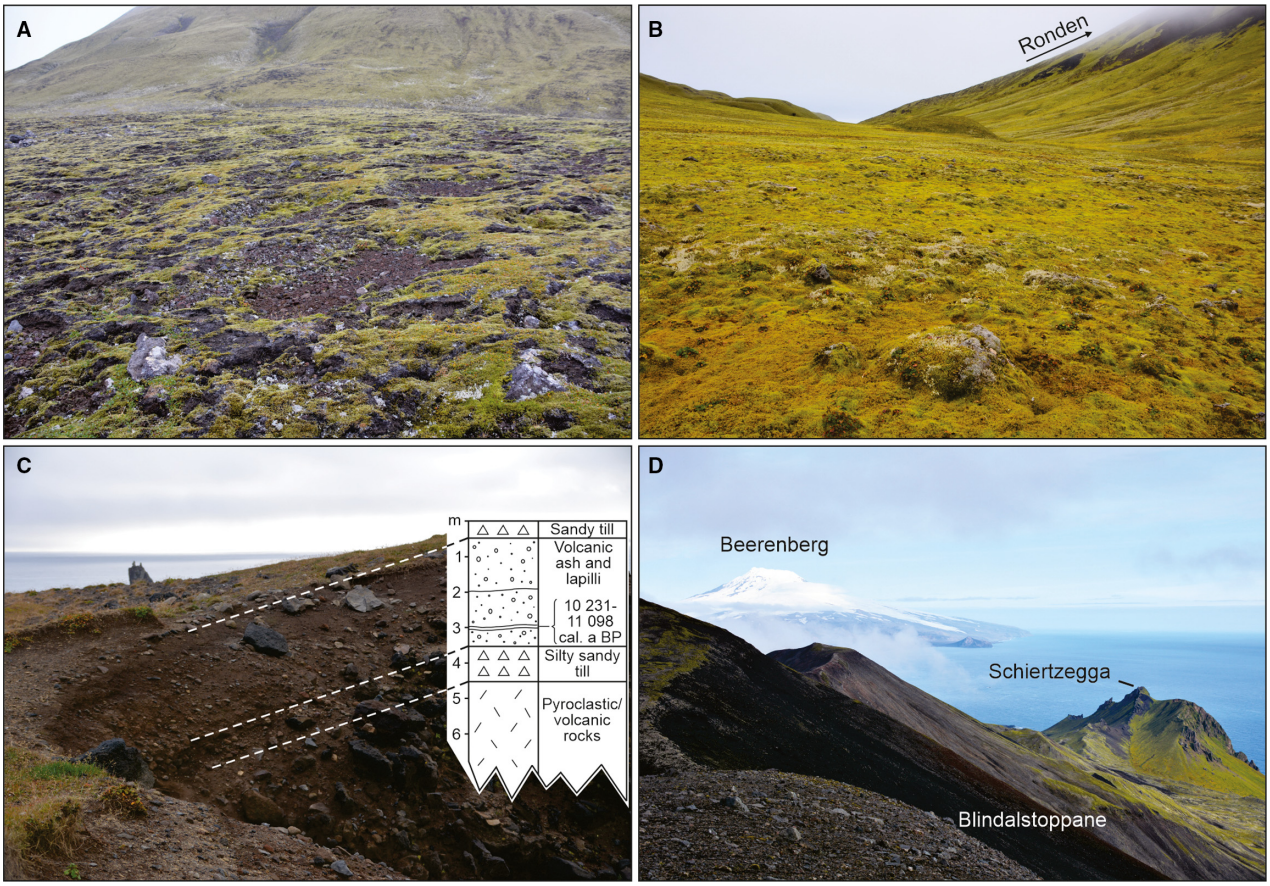

Fig. 11. Glacial deposits in Sør-Jan. For location of sites, see Fig. 2B. A. Thick till just east of Vøringen. B. Thick till southeast of Ronden. C. Section at Kapp Wien where till covers the top and organic material occur in volcanic deposits ~3 m below the surface. Radiocarbon age of the organic material is shown in the sedimentary log. D. Thin cover of till at Blindalstoppane (in the foreground of the photograph). [Colour figure can be viewed at www.boreas.dk]

exposed during the LGM sea-level lowstand (Fig. 15A). Assuming a sea-level lowstand of –125 m (Clark & Tarasov 2014), the coastline during the LGM may have been as shown in Fig. 15A; however, this does not account for local glacio-isostatic effects and postglacial submarine volcanism that may have altered the landscape.

Regardless of the maximum extent of the LGM ice cap, some assumptions concerning former surface profiles and, thus, glacier geometry may be made. In the north, around Mount Beerenberg, topography is very steep and water depths exceeding 1000 m are present less than 5 km from the coast, which likely resulted in intensive calving. Thus, ice thickness over Mount Beerenberg may not have been very much different from today.

Shallow areas with water depths between 10 and 100 m in coastal waters to the southeast and south may have allowed further expansion and therefore thicker ice to form, possibly resulting in a glacier profile such as that shown in Fig. 15B. This raises the possibility for two, or perhaps three, spreading centres during the LGM, one over Mount Beerenberg and a second or third coalescing over the remaining high ground to the south as well as the adjacent shallow submarine areas. Despite a lack of geological or geomorphological data, we suggest that, based on glaciological constraints and considerations, the ice growth over Mount Beerenberg was limited by calving. Similarly, we suggest that southern Jan Mayen supported the thickest glacier ice, which is independently supported by our observations of till cover at the highest elevations. One consequence of this conceptual model of the former ice cap is that there was apparently a low saddle between the northern and southern centres of ice growth (Fig. 15B).

Age of the Jan Mayen ice cap and its deglaciation

A set of K-Ar and $^{40}Ar/^{39}Ar$ dates of volcanic rocks underlying till (Fig. 13) was used to provide a maximum-limiting age for the local inception of the last glaciation. As one might expect, the spread in the obtained ages is quite large. The youngest age representing a preglacial eruption, 47±6.3 ka, is much older than inferred inception ages in other areas such as Greenland, western Norway, and the continental shelf in the North Sea. Ice growth during late MIS 3 and early MIS 2 is indicated

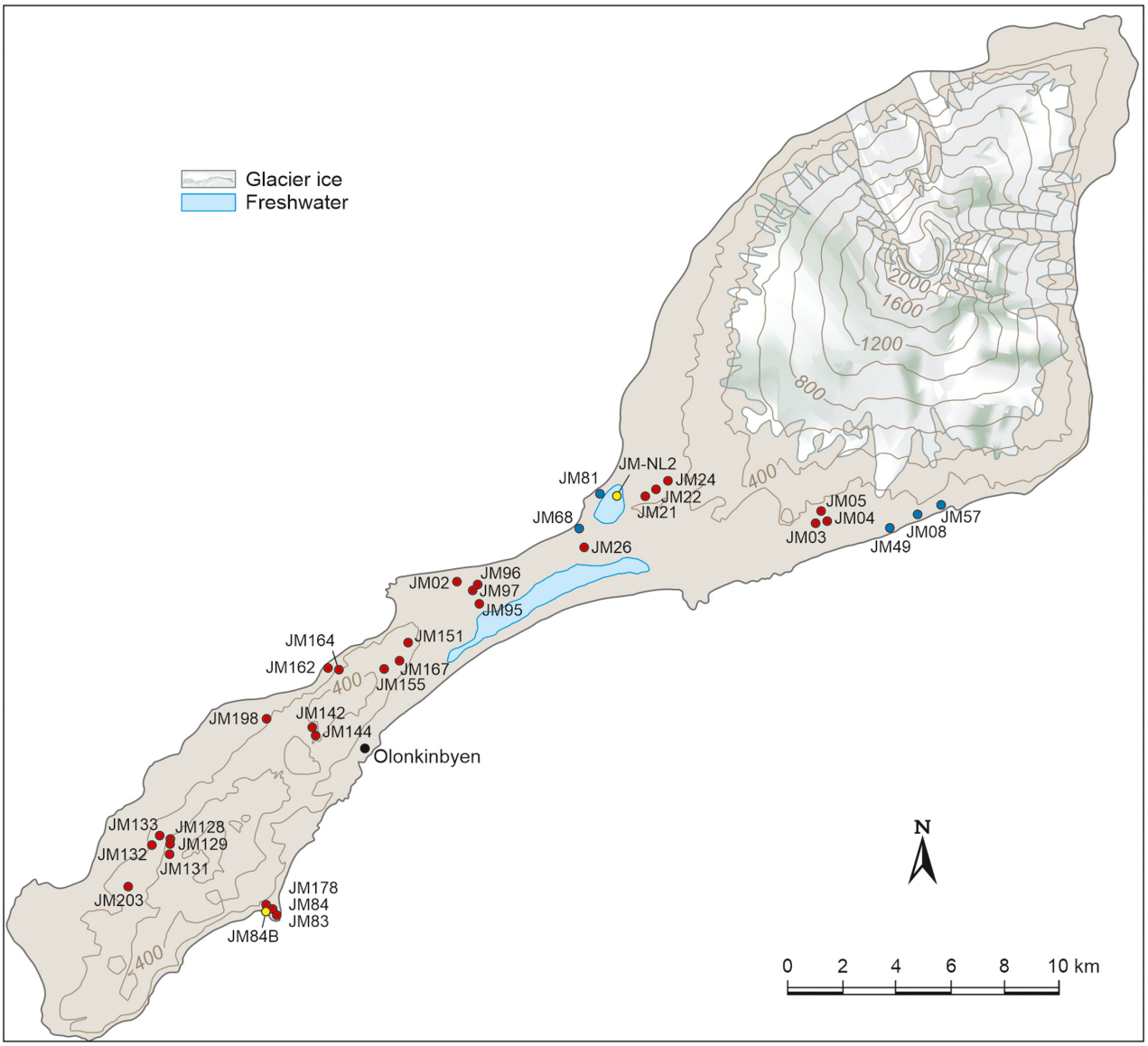

Fig. 12. Location of the sites sampled for TCN (red circles), K-Ar and $^{40}Ar/^{39}Ar$ (blue circles), and ^{14}C (yellow circles) dates. Site numbers shown are given in Tables 1, 2 and 3 with the corresponding ages. Topography is shown with 200 m contour interval. [Colour figure can be viewed at www.boreas.dk]

from ice-cores in Greenland (GISP2, Meese *et al.* 1997; NGRIP, NGRIP Members 2004). In western Norway, key stratigraphical localities in caves containing deposits of the Ålesund Interstadial (Mangerud *et al.* 2010) constrain ice inception there to sometime after 34–28 ^{14}C ka BP (Larsen *et al.* 1987; Valen *et al.* 1995). Ice-free marine conditions with ameliorated climate preceding the LGM are also indicated in the North Sea (east of Shetland) during the time interval 39–29 ka (Sejrup *et al.* 2009). The Kapp Håp section, from where the youngest age was obtained (Table 1, Fig. 13), is located only 1–2 km distal to the present ice margin, and 2.5 km east of a large LIA moraine. Till in this locality may, therefore, not necessarily imply a former ice cap of substantially greater extent than that of the LIA. Alternatively, the northern part of the island may have been glaciated much earlier (and for a longer period) than the lower areas to the south. Having said that, we suggest that it is likely that the main phase of ice cap growth on Jan Mayan was penecontemporaneous with the onset of glacial expansion in the surrounding North Atlantic, i.e. after 34 ka (Fig. 16). The geographical setting of Jan Mayen, far out in the Norwegian-Greenland Sea (Fig. 1) and surrounded by Arctic and Polar water-masses with available moisture, supports this assumption.

According to Clark *et al.* (2009), global growth of the last ice sheets towards their maximum extent occurred

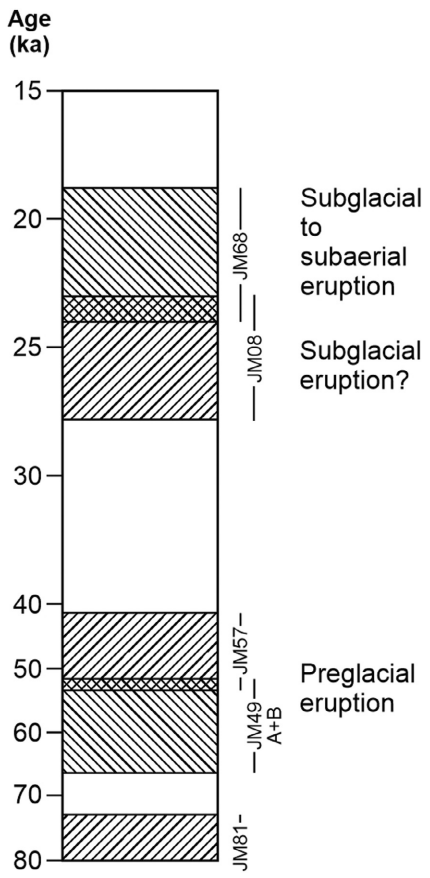

Fig. 13. Results of the K-Ar and $^{40}Ar/^{39}Ar$ dating, see Table 1 for more details. Geological interpretation to the right of the column.

between 33.0 and 26.5 ka, in response to decreases in northern summer insolation, sea surface temperatures, and atmospheric CO_2 concentrations. Most ice sheets reached their maximum position between 26.5 and 19–20 ka. The timing of their maximum positions is, however, highly variable, even for different regions of the same ice sheet (e.g. Hughes *et al.* 2016; Larsen *et al.* 2016).

Some suggestions regarding the age of the maximum position of the Jan Mayen ice cap can be made, despite an absence of direct ages for known or hypothesized maximum ice margins. K-Ar samples from two sites yielded maximum-limiting ages for subsequent intervals of glacial inundation. Kapp Fishburn (Fig. 2B), a volcanic dyke interpreted to have formed when the area was ice-covered, is dated to 25.4±2.4 ka (Table 1, Figs 13, 15). The mountain Domen (Figs 2B, 8B) started to form subglacially, before protruding through the ice surface. K-Ar data suggest that this eruption occurred at 21.5±2.6 ka (Table 1, Figs 13, 15), which may be considered as a close constraint for deglaciation. From the available data, we can only say that the ice cap achieved its maximum extent sometime before 21.5±2.6 ka and after 47.6±6.3 ka. This is in agreement with results from surrounding regions, such as the western continental shelf of Iceland where the maximum glacier position was reached at or just after *c.* 24 cal. ka BP (20 ^{14}C ka BP, Norðdahl & Pétursson 2005), or in the North Sea where the British–Irish Ice Sheet reached its maximum *c.* 26–25 ka BP (Bradwell *et al.* 2019). Moreover, ice dome thinning in northern and western Spitsbergen seems to have started between *c.* 26±2.3 and 20.1±1.6 ka (Gjermundsen *et al.* 2013; Hormes *et al.* 2013), suggesting a maximum position just prior to this, which is in line with the ages of mass transported debris on the western Svalbard slope, indicating a fully glaciated shelf at *c.* 24 ka BP (Rasmussen *et al.* 2007; Jessen *et al.* 2010).

The oldest deglaciation ages we obtained are six TCN ages from Sør-Jan (Svartfjellet and Breidfjellet) and Midt-Jan (Mohnberget and Lågheia), which range between 23.1 and 19.5 ka (Fig. 14). The most southerly of these, from Breidfjellet, yielded an age of 23.1±3.6 ka (Table 2, Fig. 14), possibly indicating that the southernmost part of Jan Mayen was deglaciated at this time, although no other dates are available to corroborate this interpretation. Five additional deglaciation ages from this region all cluster between 21.4 and 19.5 ka, which we consider our best estimate for widespread deglaciation on Sør-Jan and Midt-Jan (Fig. 16). The TCN ages are supported by our interpretation that the K-Ar date from Domen of 21.5±2.6 ka is close to the age of deglaciation. Furthermore, from the area close to Domen, resedimented terrestrial plant fragments collected from a lake core from Nordlaguna were dated to 16 028–17 035 cal. a BP (Table 3, Fig. 16), indicating that vegetation was established by this time. Based on all these data we conclude that deglaciation was underway at 21.5–19.5 ka. This would indicate that deglaciation on Jan Mayen was penecontemporaneous with other areas in the North Atlantic region. As mentioned, ice dome thinning over Spitsbergen might have started as early as 26 ka; however, increased thinning of the Svalbard-Barents Sea ice sheet leading to rapid deglaciation from the outer shelf took place sometime later, around 24 ka BP (Bauch *et al.* 2001; Jessen & Rasmussen 2019). In the Greenland Sea, just NNW of Jan Mayen, deglaciation likely started later, around 19–18 ka, with freshwater discharge directly from the Greenland Ice Sheet (Telesiński *et al.* 2014, 2015). Farther south, rapid deglaciation of the western and northern shelf of Iceland started around 18.6 ka BP (Andrews *et al.* 2000). New results from the western shelf of Shetland indicate initial ice-sheet retreat after 24.8 and before 23.8 ka BP (Bradwell *et al.* 2019), and initial glacier retreat across the Dogger Bank was complete by 23.1 ka (Roberts *et al.* 2018). Cosmogenic ^{10}Be ages from the outer coast of SW Norway, in the path of the Norwegian Channel Ice Stream (NCIS), suggest retreat about 22.0±2.0–20.0±0.7 ka for the NCIS (Svendsen *et al.* 2015). An

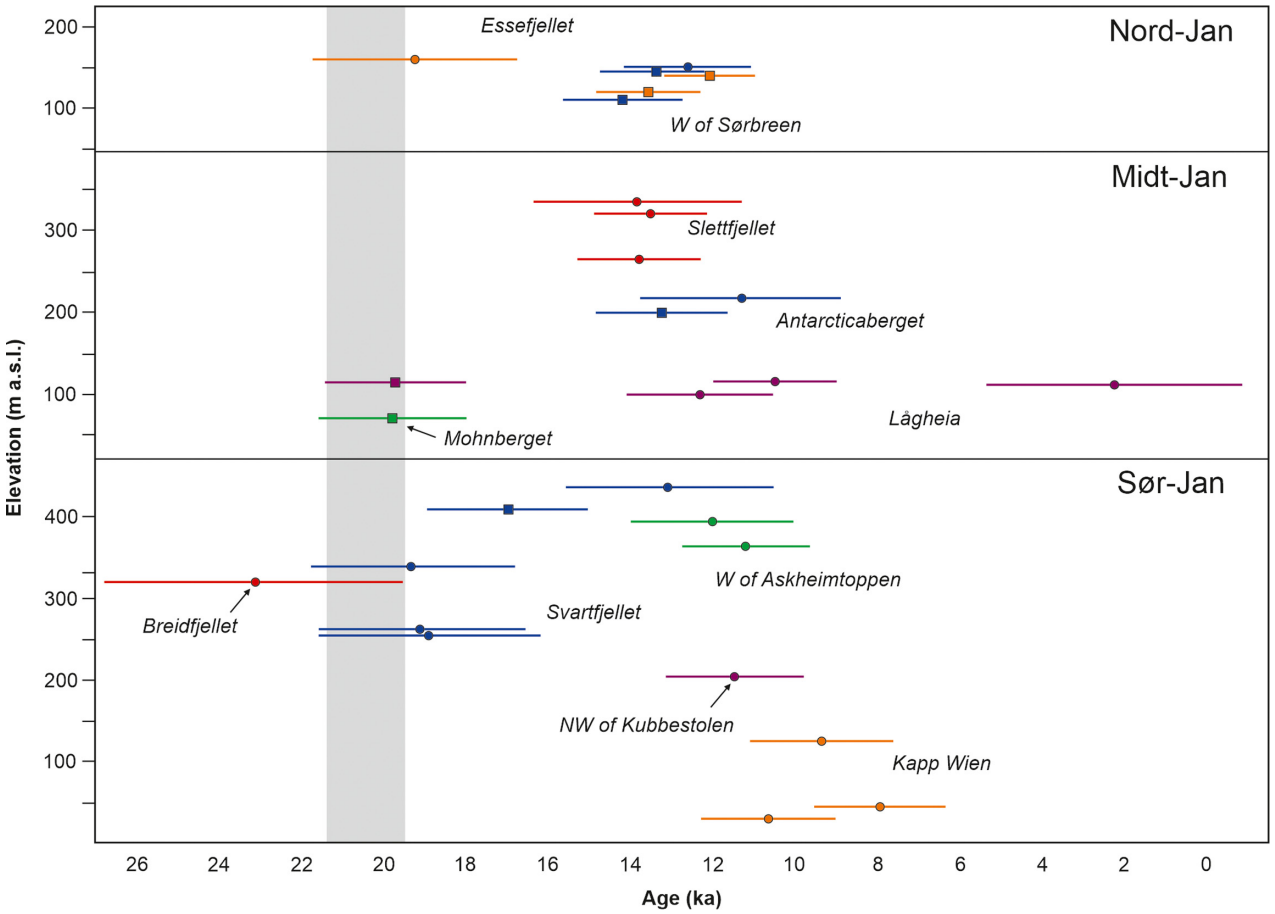

Fig. 14. Results of the TCN dating plotted against elevation for the three regions Sør-Jan, Midt-Jan and Nord-Jan. For local place names, see Fig. 2B. Dates are marked with squares (bedrock) and circles (block on till). Different colours are only used to distinguish the different geographical areas from each other. The grey bar represents the oldest deglaciation age interval (21.4–19.5 ka) as implied by the dates. [Colour figure can be viewed at www.boreas.dk]

initial deglaciation of around 21.5–19.5 ka in Jan Mayen thus fits well with the suggested deglaciation ages from surrounding regions.

Given the relatively small chronological data set for Jan Mayen, the detailed pattern of deglaciation is difficult to establish (Fig. 14). In Sør-Jan it seems that deglaciation started at elevations of around 250–350 m a.s.l. and close to the coastal cliffs of Svartfjellet and Breidfjellet (cf. Fig. 10C, E). In contrast, the coastal site at Kapp Wien yielded TCN ages younger than 11 ka (Fig. 14, Table 2); however, subtill organic material in a section dating to 10 231–11 098 cal. a BP (Fig. 11C, Table 3) may indicate that the exposure ages actually record deglaciation after a Younger Dryas advance rather than initial deglaciation following the LGM (Fig. 16).

Except for the TCN ages at Kapp Wien, the other younger ages in Sør- and Midt-Jan, which span *c.* 14 to 10 ka (Fig. 14) cannot be unambiguously interpreted as recording a pre-Younger Dryas deglaciation and subsequent Younger Dryas re-advance. The dates should likely be interpreted as recording gradual ice-marginal retreat and glacier thinning. We suggest that the ages of 11.2±1.5 and 12.0±2 ka from the westward-facing valley area west of Askheimtoppen, at almost 400 m a.s.l. (Fig. 2B), record the timing of the deglaciation. The southward-facing Kapp Wien site might have been deglaciated earlier and later overridden by a Younger Dryas glacier re-advance; however, further studies need to be undertaken to confirm this hypothesis.

In Nord-Jan, the oldest TCN age is from a boulder on till at Essefjellet on the SW flank of Mount Beerenberg (19.2±2.5 ka, Table 2, Fig. 14). Such an early deglaciation correlates well with the radiocarbon age on terrestrial plant materials in Nordlaguna (located ~2 km from Essafjellet), indicating deglaciation before 17–16 cal. ka BP (Fig. 16). However, this scenario conflicts with the two remaining TCN ages from Essefjellet and three TCN ages from nearby Slettfjellet, which are <13.8 ka. SW of Sørbreen, a block on till also yields a younger age

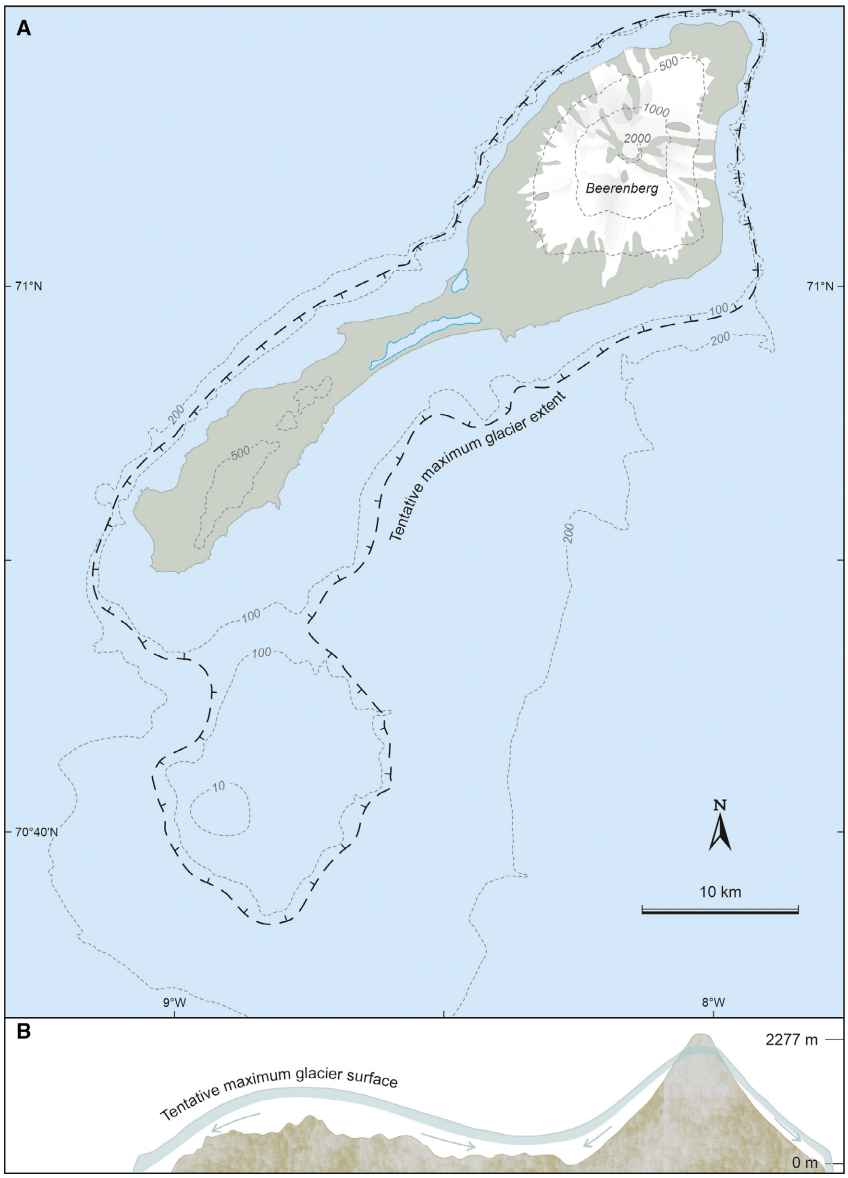

Fig. 15. A. Probable maximum extent of the Late Weichselian ice cap of Jan Mayen, approximated by the ~125 m bathymetric contour surrounding the island. The suggested extent is based on (i) documentation that the glacier was beyond the present coastline, (ii) documentation that the glacier covered the highest peaks in Sør-Jan, and (iii) assuming that the glacier-covered shallow areas on the shelf during the eustatic low sea level. B. Idealized S–N profile of the Late Weichselian ice cap maximum based on A and the bathymetric and topographic data. [Colour figure can be viewed at www.boreas.dk]

(12.6±1.5 ka), whereas two bedrock exposures date to 14.3±1.5 and 13.4±1.4 ka (Table 2, Fig. 14). We suspect that the deglaciation in Nord-Jan was delayed on the order of a few millennia compared to Midt- and Sør-Jan, and that ice-marginal retreat was not fully underway until around 14 ka.

Initial deglaciation in Jan Mayen at 21.5–19.5 ka is probably linked to increased northern summer insolation from about 22 ka (Laskar *et al.* 2004), which, according to Clark *et al.* (2009), was the primary triggering mechanism for the onset of deglaciation in the Northern Hemisphere. The physiography of Jan Mayen (i.e. area, hypsometry, shape; Fig. 15), may have rendered the former ice cap prone to marine downdraw, especially in Nord-Jan where deglaciation may have been delayed compared to Midt- and Sør-Jan. We suspect that Nord-Jan during this time was occupied by ice mass at least as large as today, and that some of the glaciers claved in to the sea. As all the youngest deglaciation dates are from sites at elevations exceeding 100 m a.s.l., except at Mohnberget which is located at 71 m a.s.l., it must be considered that the timing and rate of ice-marginal retreat was affected by

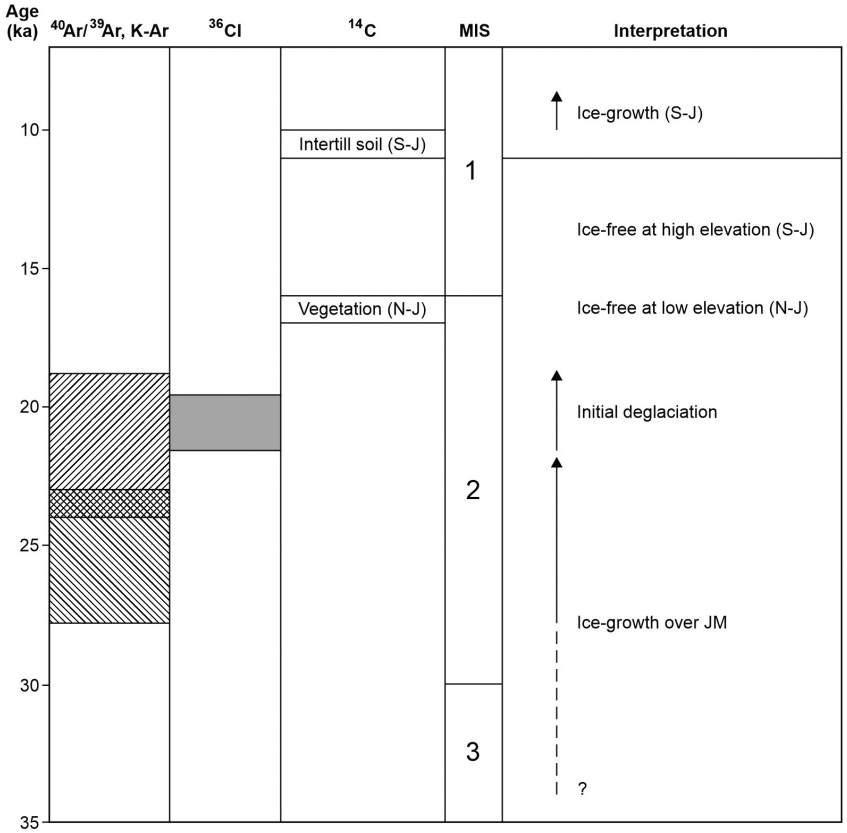

Fig. 16. Late Weichselian glacier history in Jan Mayen. Chronology is based on K- and $^{40}Ar/^{39}Ar$, TCN and ^{14}C dating results. S-J = Sør-Jan; N-J = Nord-Jan; JM = Jan Mayen. See text for discussion.

a rise in relative sea level. In Iceland, although deglaciation occurred somewhat later (around 18.6 ka BP at the shelf west and north of Iceland), the ice sheet retreated rapidly from the shelf after 15–14.7 ka BP, mainly controlled by rising global sea level and a collapse of the marine-based sector (Ingólfsson & Norðdahl 2001; Norðdahl & Ingólfsson 2015). Even though local glacio-isostatic adjustments in Jan Mayen are still unknown, one may infer a similar scenario for Jan Mayen.

The data presented here suggest a link between initial deglaciation, i.e. crustal unloading, and volcanic eruptions on Jan Mayen. The formation of Domen (Fig. 8B), which started to form subglacially and eventually protruded through the ice surface around 21.5 ka, may have been triggered by crustal unloading during deglaciation. Tindar close to Pukkelryggen, with its nearby meltwater channels (Fig. 9D), and the deep meltwater channel at Lågheia incised through a thick succession of volcanic ash (Fig. 9C), both indicate volcanic eruption with ash fall on the former glacier surface. These features, in addition to the numerous lavas, domes, and tephra of unknown ages (Fig. 4), may be linked to crustal unloading and an intensified pulse of volcanic activity in Jan Mayen. However, this hypothesis needs to be tested with additional geomorphological mapping and the establishment of a more robust chronology.

Conclusions

We have integrated glacial deposits and landforms, stratigraphy, and a new chronological data set to reconstruct the glacial history of Jan Mayen. We have focused on determining the former extent of the ice cap and the timing of its growth and early decay during the Late Weichselian. Our main findings are:

- The entire island of Jan Mayen was covered by a continuous ice cap during the Late Weichselian.
- In Nord-Jan where glaciers exist at present, the Late Weichselian ice cap advanced to the steep coast and terminated at a calving tidewater margin.
- Sør- and Midt-Jan were covered by glacier ice during Late Weichselian time, and the ice cap likely extended onto the shallow marine areas southeast and east of the island.
- The Late Weichselian ice cap was likely thicker over Sør- and Midt-Jan than over Nord-Jan.

- Expansion of the Late Weichselian ice cap started sometime after approximately 47 ka, though potentially after 34 ka according to stratigraphical data from other North Atlantic regions.
- The maximum extent of the Jan Mayen ice cap was attained sometime before 21.5±2.6 ka, and deglaciation was underway 21.5–19.5 ka.
- In Sør-Jan, deglaciation started at elevations above 200 m a.s.l. and by ~14.0–13.5 ka most of Sør- and Midt-Jan were deglaciated.
- The deglaciation may have started later in Nord-Jan than in the south, but by 17–16 cal. a BP vegetation was established on the coastal southern flank of Mount Beerenberg.

Acknowledgements. – Financial support was given by the Geological Survey of Norway, The Research Council of Norway (Grant No. 244135/E10), personal grants to A. Lysså through the Arctic Field Grant 2014 (Research Council of Norway, RIS-ID-ES538785) and through The Royal Norwegian Society of Sciences and Letters (2019, DKNVS). Logistical support, and necessary permissions, were provided by the County Governor of Nordland and the Norwegian Defence Logistic Organisation (CYFOR, Jan Mayen). The Norwegian Polar Institute and Kongsberg Satellite Services provided aerial orthophotos and satellite images, respectively. Irene Lundquist helped with the graphics. Ruikai Xie from NGU Laboratory is thanked for potassium determinations. Nasim Mozafari, Serdar Yeşilyurt and Juliana Krbanjevic at the Institute of Geological Sciences, Bern University, greatly contributed to the sample preparation for cosmogenic ^{36}Cl analysis. Personnel and staff at the Jan Mayen Station and Torgeir Madsen at CYFOR Jan Mayen kindly supported us with their hospitality, friendship, and shared leisure time, through many field seasons. Before the first field trip, fruitful discussions and good advice were given by Jan Mangerud who visited the island in the 1970s. Thomas Lakeman improved the English language and provided constructive comments. Anna Hughes and Vincent Rinterknecht reviewed and gave constructive suggestions to the manuscript. To all these institutions and persons, we extend our sincere thanks.

Author contributions. – AL and EAL conceived and designed the project and carried out all the fieldwork, with a total of 33 weeks fieldwork over 5 years. JA took part in the fieldwork for 1 week in 2015, prepared the TCN samples, calculated the cosmogenic exposure ages, and helped with interpretation of the ages. NA and CV performed the ^{36}Cl measurements. MG and RvdL calculated and interpreted the ^{40}Ar/^{39}Ar and K-Ar ages. AH contributed with field observations from the 1970s. AL wrote the manuscript with input from all authors.

References

Anda, E., Orheim, O. & Mangerud, J. 1985: Late Holocene glacier variations and climate at Jan Mayen. *Polar Research 3*, 129–140.

Andrews, J. T., Harðardóttir, J., Helgadóttir, G., Jennings, A. E., Geirsdóttir, A., Sveinsbjörnsdóttir, A. E., Schoolfield, S., Kristjánsdóttir, G. B., Smith, L. M., Thors, K. & Syvitski, J. 2000: The N and W Iceland Shelf: insight into Last Glacial Maximum ice extent and deglaciation based on acoustic stratigraphy and basal radiocarbon AMS dates. *Quaternary Science Reviews 19*, 619–631.

Bauch, H. A., Erlenkeuser, H., Spielhagen, R. F., Struck, U., Matthiessen, J., Thiede, J. & Heinemeier, J. 2001: A multiproxy reconstruction of the evolution of deep and surface waters in the subarctic Nordic seas over the last 30,000 yr. *Quaternary Science Reviews 20*, 659–678.

Blischke, A., Gaina, C., Hopper, J. R., Péron-Pinvidic, G., Brandsdóttir, B., Guarnieri, P., Erlendsson, Ö. & Gunnarsson, K. 2016: The Jan Mayen microcontinent: an update of its architecture, structural development and role during the transition from the Ægir Ridge to the mid-oceanic Kolbeinsey Ridge. *Geological Society, London, Special Publications 447*, 299–337.

Bradwell, T., Small, D., Fabel, D., Clark, C. D., Chiverrell, R. C., Saher, M. H., Dove, D., Callard, S. L., Burke, M. J., Moreton, S. G., Medialdea, A., Bateman, M. D., Roberts, D. H., Golledge, N. R., Finlayson, A., Morgan, S. & Ó Cofaigh, C. 2019: Pattern, style and timing of British-Irish Ice Sheet retreat: Shetland and northern North Sea sector. *Journal of Quaternary Science*, https://doi.org/10.1002/jqs.3163.

Carstens, H. 1962: Lavas of the southern part of Jan Mayen. *Norsk Polarinstitutt, Årbok 1961*, 69–82.

Christl, M., Vockenhuber, C., Kubik, P. W., Wacker, L., Lachner, J., Alfimov, V. & Synal, H. A. 2013: The ETH Zurich AMS facilities: performance parameters and reference materials. *Nuclear Instruments and Methods B 294*, 29–38.

Clark, P. U. & Tarasov, L. 2014: Closing the sea level budget at the Last Glacial Maximum. *Proceedings of the National Academy of Sciences USA 111 (45)*, 15861–15862.

Clark, P. U., Dyke, A. S., Shakum, J. D., Carlson, A. E., Clark, J., Wohlfarth, B., Mitrovica, J. X., Hostetler, S. W. & McCabe, A. M. 2009: The Last Glacial Maximum. *Science 325*, 710–714.

Cromwell, G., Tauxe, L., Staudigel, H., Constable, C. G., Koppers, A. A. P. & Pedersen, R.-B. 2013: In search of long-term hemispheric asymmetry in the geomagnetic field: results from high northern latitudes. *Geochemistry, Geophysics, Geosystems 14*, 3234–3249.

Dallmann, W. K. 1997: Bergrunnsgeologi Jan Mayen. *In* Gabrielsen, G. W., Brekke, B., Alsos, I. G. & Hansen, J. R. (eds.): *Natur og kulturmiljøet på Jan Mayen – med en vurdering av verneverdier, kunnskapsbehov og forvaltning*, p. 35. *Norsk Polarinstitutt, Meddelelser 144*.

Dunne, J., Elmore, D. & Muzikar, P. 1999: Scaling factors for the rates of production of cosmogenic nuclides for geometric shielding and attenuation at depth on sloped surfaces. *Geomorphology 27*, 3–11.

Eldholm, O. & Sundvor, E. 1980: The continental margins of the Norwegian-Greenland Sea: recent results and outstanding problems. *Philosophical Transactions of the Royal Society of London A 294*, 77–86.

Fitch, F. J. 1964: The development of the Beerenberg volcano, Jan Mayen. *Proceedings of the Geologists Association 75 (2)*, 133–165.

Fitch, F., Grasty, R. & Miller, J. 1965: Potassium-argon ages of rocks from Jan Mayen and an outline of its volcanic history. *Nature 207*, 1349–1351.

Funder, S., Kjeldsen, K. K., Kjær, K. H. & Ó Cofaigh, C. 2011: The Greenland ice sheet during the past 300,000 years: a review. *In* Ehlers, J., Gibbard, P. L. & Hughes P. D. (eds.): *Quaternary Glaciations. Extent and Chronology*, 699–713. *Developments in Quaternary Science 15*. Elsevier, Amsterdam.

Gjermundsen, E. F., Briner, J. P., Akçar, N., Salvigsen, O., Kubik, P., Gantert, N. & Hormes, A. 2013: Late Weichselian local ice dome configuration and chronology in Northwestern Svalbard: early thinning, late retreat. *Quaternary Science Reviews 72*, 112–127.

Hałas, S. & Wójtowicz, A. 2014: Propagation of error formulas for K-Ar dating method. *Geochronometria 41*, 202–206.

Hormes, A., Gjermundsen, E. F. & Rasmussen, T. L. 2013: From mountain top to the deep sea – deglaciation in 4D of the northwestern Barents Sea ice sheet. *Quaternary Science Reviews 75*, 78–99.

Hudson, S. R., Gjelten, H. M., Isaksen, K. & Kohler, J. 2019: An assessment of MOSJ. Environmental status for atmospheric and terrestrial climate in Svalbard and Jan Mayen. *Norwegian Polar Institute, Report 050*, 42 pp.

Hughes, A. L. C., Gyllencreutz, R., Lohne, Ø. S., Mangerud, J. & Svendsen, J. I. 2016: The last Eurasian ice sheets – a chronological database and time-slice reconstruction, DATED-1. *Boreas 45*, 1–45.

Imsland, P. 1978: The Geology of the Volcanic Island Jan Mayen, Arctic Ocean, *Nordic Volcanological Institute 78,* 74 pp.

Ingólfsson, Ó. & Landvik, J. Y. 2013: The Svalbard – Barents Sea ice-sheet – Historical, current and future perspectives. *Quaternary Science Reviews 64*, 33–60.

Ingólfsson, Ó. & Norðdahl, H. 2001: High relative sea-level during the Bölling Interstadial in Western Iceland: a reflection of ice-sheet collapse and extremely rapid glacial unloading. *Arctic, Antarctic and Alpine Research 33*, 231–243.

Ivy-Ochs, S., Synal, H. A., Roth, C. & Schaller, M. 2004: Initial results from isotope dilution for Cl and ^{36}Cl measurements at the PSI/ETH Zurich AMS facility. *Nuclear Instruments and Methods B 223–224*, 623–627.

Jakobsson, S. P. & Gudmundsson, M. T. 2008: Subglacial and intraglacial volcanic formations in Iceland. *Jökull 58*, 179–196.

Jessen, S. P. & Rasmussen, T. L. 2019: Ice-rafting patterns on the western Svalbard slope 74-0 ka: interplay between ice-sheet activity, climate and ocean circulation. *Boreas 48*, 236–256.

Jessen, S. P., Rasmussen, T. I., Nielsen, T. & Solheim, A. 2010: A new Late Weichselian and Holocene marine chronology for the western Svalbard slope 30,000-0 cal years BP. *Quaternary Science Reviews 29*, 1301–1312.

Larsen, E., Fredin, O., Lysså, A., Amantov, A., Fjeldskaar, W. & Ottesen, D. 2016: Causes of time-transgressive glacial maxima positions of the last Scandinavian Ice Sheet. *Norwegian Journal of Geology 96*, 159–170.

Larsen, E., Gulliksen, S., Lauritzen, S.-E., Lie, R., Løvlie, R. & Mangerud, J. 1987: Cave stratigraphy in western Norway; multiple Weichselian glaciations and interstadial vertebrate fauna. *Boreas 16*, 267–292.

Laskar, J., Robutel, P., Joutel, F., Gastineau, M., Correia, A. C. M. & Levrard, B. 2004: A long-term numerical solution for the insolation quantities of the Earth. *Astronomy & Astrophysics 428*, 261–285.

Lee, J. Y., Marti, K., Severinghaus, J. P., Kawamura, K., Yoo, H. S., Lee, J. B. & Kim, J. S. 2006: A redetermination of the isotopic abundances of atmospheric Ar. *Geochimica et Cosmochimica Acta 70*, 4507–4512.

Licciardi, J. M., Denoncourt, C. L. & Finkel, R. C. 2008: Cosmogenic ^{36}Cl production rates from Ca spallation in Iceland. *Earth and Planetary Science Letters 267*, 365–377.

Mangerud, J., Gulliksen, S. & Larsen, E. 2010: ^{14}C-dated fluctuations of the western flank of the Scandinavian Ice Sheet 45-25 kyr BP compared with Bølling-Younger Dryas fluctuations and Dansgaard-Oeschger events in Greenland. *Boreas 39*, 328–342.

Mangerud, J., Gyllencreutz, R., Lohne, Ø. & Svendsen, J. I. 2011: Glacial history of Norway. *In* Ehlers, J., Gibbard, P. L. & Hughes, P. D. (eds). *Quaternary Glaciations. Extent and Chronology*, 279–298. *Developments in Quaternary Science 15*. Elsevier, Amsterdam.

Marrero, S. M., Phillips, F. M., Caffeee, M. W. & Gosse, J. C. 2016: CRINUS-Earth cosmogenic ^{36}Cl calibration. *Quaternary Geochronology 31*, 199–219.

Meese, D. A., Gow, A. J., Alley, R. B., Zielinski, G. A., Grootes, P. M., Ram, M., Taylor, K. C., Mayewski, P. A. & Bolzan, J. F. 1997: The GISP2 depth-age scale: methods and results. *Journal of Geophysical Research 102 (C12) 26*, 411–424.

Mozafari, N., Tikhomirov, D., Sumer, Ö., Özkaymak, Ç., Uzel, B., Yeşilyurt, S., Ivy-Ochs, S., Vockenhuber, C., Sözbilir, H. & Akçar, N. 2019: Dating of active normal fault scarps in the Büyük Menderes Graben (western Anatolia) and its implications for seismic history. *Quaternary Science Reviews 220*, 111–123.

NGRIP Members 2004: High resolution climate record of the northern hemisphere reaching into the last interglacial period. *Nature 431*, 147–151.

Norðdahl, H. & Ingólfsson, Ó. 2015: Collapse of the Icelandic ice sheet controlled by sea-level rise? *Arktos 1*, 13, https://doi.org/10.1007/s41063-015-0020-x.

Norðdahl, H. & Pétursson, H. G. 2005: Relative sea-level changes in Iceland. New aspects of the Weichselian deglaciation of Iceland. *In* Caseldine, C., Russel, A., Harðardóttir, J. & Knudsen, O. (eds.): *Iceland – Modern Processes and Past Environments*, 25–78. Elsevier, Amsterdam.

Orheim, O. 1993: Glaciers of Jan Mayen, Norway. *In* Williams R. S. & Ferringo, J. G. (eds.): *Satellite Image Atlas of Glaciers of the World. Glaciers of Europe. U.S. Geological Survey Professional Paper 1386-E-6*.

Plunder, A., Bandyopadhyay, D., Ganerød, M., Advokaat, E. L., Ghosh, B., Pandopadhyay, P. & van Hinsbergen, D. J. J. 2020: History of subduction polarity reversal during arc-continent collision: constraints from the Andaman Ophiolite and its metamorphic sole. *Tectonics, American Geophysical Union*, https://doi.org/10.1029/2019tc005762.

Polyak, L., Alley, R. B., Andrews, J. T., Brigham-Grette, J., Cronin, T. M., Darby, D. A., Dyke, A. S., Fitzpatrick, J. J., Funder, S., Holland, M., Jennings, A. E., Miller, G. H., O`Reagan, M., Savelle, J., Serreze, M., St John, K., White, J. W. C. & Wolff, E. 2010: History of sea ice in the Arctic. *Quaternary Science Reviews 29*, 1757–1778.

Porter, C., Morin, P., Howat, I., Noh, M.-J., Bates, B., Peterman, K., Keesey, S., Schlenk, M., Gardiner, J., Tomko, K., Willis, M., Kelleher, C., Cloutier, M., Husby, E., Foga, S., Nakamura, H., Platson, M., Wethington, M. Jr, Williamson, C., Bauer, G., Enos, J., Arnold, G., Kramer, W., Becker, P., Doshi, A., D'Souza, C., Cummens, P., Laurier, F. & Bojesen, M. 2018: "*ArcticDEM*", *Harvard Dataverse*, V1, https://doi.org/10.7910/dvn/ohhukh (accessed 02.02.2017).

Rasmussen, T. I., Thomsen, E., Ślubowska, M. A., Jessen, S., Solheim, A. & Koç, N. 2007: Paleoceanographic evolution of the SW Svalbard margin (76°N) sine 20,000 ^{14}C yr BP. *Quaternary Research 67*, 100–114.

Reimer, P., Bard, E., Bayliss, A., Beck, J. W., Blackwell, P. G., Ramsey, C. B., Buck, C. E., Cheng, H., Edwards, R. L., Friedrich, M., Grootes, P. M., Guilderson, T. G., Haflidason, H., Hajdas, I., Hatte, C., Heaton, T. J., Hoffmann, D. L., Hogg, A. G., Hughen, K. A., Kaiser, K. F., Kromer, B., Manning, S. W., Niu, M., Reimer, R. W., Richards, D. A., Scott, E. M., Southon, J. R., Staff, R. A., Turney, C. S. M. & van der Plicht, J. 2013: IntCal13 and Marine 13 radiocarbon age calibration curves 0-50,000 years cal BP. *Radiocarbon 55*, 1869–1887.

Roberts, D. H., Evans, D. J. A., Callard, S. L., Clark, C. D., Bateman, M. D., Medialdea, A., Dove, D., Cotterill, C. J., Saher, M., Ó Cofaigh, C. O., Chiverrell, R. C., Moreton, S. G., Fabel, D. & Bradwell, T. 2018: Ice marginal dynamics of the last British-Irish Ice Sheet in the southern North Sea: Ice limits, timing and the influence of the Dogger Bank. *Quaternary Science Reviews 198*, 181–207.

Rodríguez-Pérez, Q. & Ottemöller, L. 2014: Source study of the Jan Mayen transform fault strike-slip earthquakes. *Tectonophysics 628*, 71–84.

Sejrup, H. P., Nygård, A., Hall, A. M. & Haflidason, H. 2009: Middle and Late Weichselian (Devensian) glaciation history of south-western Norway, North Sea and eastern UK. *Quaternary Science Reviews 28*, 370–380.

Siggerud, T. 1972: The volcanic eruption of Jan Mayen, 1970. *Norsk Polarinstitutt Årbok 1970*, 5–18.

Siggerud, T. 1986: Jan Mayen stadig en aktiv vulkan: litt om utbruddet i 1985 og annen vulkanaktivitet. *Polarboken 1985–1986*, 105–109.

Sørensen, B. M., Ottemöller, L., Havskov, J., Atakan, K., Hellevang, B. & Pedersen, R. B. 2007: Tectonic process in the Jan Mayen fracture zone based on earthquake occurrence and bathymetry. *Bulletin of the Seismological Society of America 97*, 772–779.

Steiger, R. H. & Jäger, E. 1977: Subcommission on geochronology: convention on the use of decay constants in geo-and cosmochronology. *Earth and Planetary Science Letters 36*, 359–362.

Stroeven, A. P., Hättestrand, C., Kleman, J., Heyman, J., Fabel, D., Fredin, O., Goodfellow, B. W., Harbor, J. M., Jansen, J. D., Olsen, L., Caffee, M. W., Fink, D., Lundqvist, J., Rosqvist, G., Strömberg, B. & Jansson, K. N. 2016: Deglaciation of Fennoscandia. *Quaternary Science Reviews 146*, 91–121.

Stuiver, M., Reimer, P. J. & Reimer, R. W. 2019: *CALIB 7.1 (WWW program)*, http://calib.org (accessed 02.04.2020).

Svendsen, J. I., Briner, J. P., Mangerud, J. & Young, N. E. 2015: Early break-up of the Norwegian Channel Ice Stream during the Last Glacial Maximum. *Quaternary Science Reviews 107*, 231–242.

Telesiński, M. M., Bauch, H. A., Spielhagen, R. F. & Kandiano, E. S. 2015: Evolution of the central Nordic Seas over the last 20 thousand years. *Quaternary Science Reviews 121*, 98–109.

Telesiński, M. M., Spielhagen, R. F. & Lind, E. M. 2014: A high-resolution Lateglacial and Holocene palaeoceanographic record from the Greenland Sea. *Boreas 43*, 273–285.

Valen, V., Larsen, E. & Mangerud, J. 1995: High-resolution paleomagnetic correlation of the Middle Weichselian ice-dammed lake sediments in two coastal caves, western Norway. *Boreas 24*, 141–153.

Vockenhuber, C., Miltenberger, K.-U. & Synal, H.-A. 2019: ^{36}Cl measurements with a gas-filled magnet at 6 MV. *Nuclear Instruments and Methods B 455*, 190–194.

Supporting Information

Additional Supporting Information may be found in the online version of this article at http://www.boreas.dk.

Table S1. K-Ar data from the samples and standards analysed in this study, Table 1.

Table S2. Geochemical composition of the ^{36}Cl samples in Table 2.